DR. BENJAMÍN FLORAN (Orcid ID : 0000-0002-3430-9335)

Article type : Research Report

Dopamine D4 receptor modulates inhibitory transmission in pallido-pallidal terminals and regulates motor behavior.

Israel Conde Rojas[a], Jackeline Acosta[b], Rene Nahum Caballero-Florán[c], Rafael Jijón-Lorenzo[a], Sergio Recillas-Morales[d], José Arturo Avalos-Fuentes[a], Francisco Paz-Bermúdez[a], Gerardo Leyva-Gómez[e], Hernán Cortés[f], Benjamín Florán[a]*

[a]*Departamento de Fisiología, Biofísica y Neurociencias. Centro de Investigación y de Estudios Avanzados del Instituto Politécnico Nacional. México*

[b]*Universidad Tecnológica de México - UNITEC MÉXICO - Campus Marina – Cuitláhuac*

[c]*Department of Pharmachology. Medical School University of Michigan.*

[d]*Faculty of Veterinary Medicine, Universidad Autónoma del Estado de México, México*

[e]*Departamento de Farmacia, Facultad de Química, Universidad Nacional Autónoma de México, Ciudad de México 04510, México.*

[f]*Laboratorio de Medicina Genómica, Departamento de Genómica, Instituto Nacional de Rehabilitación Luis Guillermo Ibarra Ibarra, Ciudad de México 14389, México*

*Corresponding author: Dr. Benjamin Florán. Departamento de Fisiología, Biofísica y Neurociencias. Centro de Investigación y de Estudios Avanzados del Instituto Politécnico Nacional.

Apartado Postal 14-740. 07000. México D.F., México Tel. +52-55-57473800 Ext. 5137; Fax: 52-55 - 57473754. *E-mail:* ***bfloran@fisio.cinvestav.mx***

Running title. *D_4R at pallido-pallidal terminals.*

ABBREVIATIONS

[^{3}H] GABA, γ-[2,3-3H(N)]-Aminobutyric acid (GABA); [^{3}H] YM-09151-2, cis-N-(1-benzyl-2-methylpyrrolidin-3-yl)-5-chloro-2-methoxy-4-methylaminobenzamide; ACSF, Artificial Cerebrospinal Fluid; AMPA, α-amino-3-hydroxy-5-methyl-4-isoxazolepropionic acid receptor; ATP-Mg, Adenosine 5′-triphosphate magnesium; AAOA, amino-oxyacetic acid; CNQX, 6-cyano-7-nitroquinoxaline-2,3-dione; D_1R, Dopamine D1 receptor(s); D_2R, Dopamine D2 receptor(s); D_4R, D3R, Dopamine D3 receptor (s); Dopamine D4 receptor(s); DL-AP-5, DL-2-amino-phosphonopentanoic acid; eIPSC, evoked inhibitory postsynaptic currents; GP, Globus pallidus; L 741,626, DL-2-amino5phosphonopentanoic acid; L 741,626, (±)-3-[4-(4-Chlorophenyl)-4-hydroxypiperidinyl]methylindole; L 745,870, (±)-3-[4-(4-Chlorophenyl)-4-hydroxypiperidinyl]methylindole; MSNs; Striatal medium-sized spiny neurons; NMDA, N-methyl-D-aspartate receptor; PD 168,077, 3-[[4-(4-Chlorophenyl)piperazin-1-yl]methyl]-1H-pyrrolo[2,3-b]pyridine hydrochloride; Quinpirole, N-[[4-(2-Cyanophenyl)-1-piperazinyl]methyl]-3-methylbenzamide maleate salt; RTN, Reticular thalamic nucleus; SDS, Sodium lauryl sulfate; SDS-PAGE, Sodium dodecyl sulfate–polyacrylamide gel electrophoresis; sIPSC, Spontaneous inhibitory postsynaptic currents; SNr, Substantia nigra pars reticulata; Sth, Subthalamic nucleus; Sulpiride, trans-(–)-(4aR)-4,4a,5,6,7,8,8a,9-Octahydro-5-propyl-1H-pyrazolo[3,4-g]quinoline monohydrochloride; Sumanirole, (S)-5-(Aminosulfonyl)-N-[(1-ethyl-2-pyrrolidinyl)methyl]-2-methoxybenzamide; TTX, Tetrodotoxin; DL-AP-5, 6-cyano-7-nitroquinoxaline-2,3-dione

ABSTRACT

Two major groups of terminals release GABA within the Globus pallidus; one group is constituted by projections from striatal neurons, while endings of the intranuclear collaterals form the other one. Each neurons' population expresses different subtypes of dopamine D2-like receptors: D_2R subtype is expressed by encephalin positive MSNs, while pallidal neurons express the D_4R subtype. The D_2R modulates the firing rate of striatal neurons and GABA release at their projection areas, while the D_4R regulates Globus pallidus neurons excitability and GABA release at their projection areas. However, it is unknown if these receptors control GABA release at pallido-pallidal collaterals and regulate motor behavior. Here, we present neurochemical evidence of protein content and binding of D_4R in pallidal synaptosomes, control of [^{3}H] GABA release in pallidal slices of rat, electrophysiological evidence of the presence of D_4R on pallidal recurrent collaterals in mouse slices, and turning behavior induced by D_4R antagonist microinjected in amphetamine challenged rats. As in projection areas of pallidal neurons, GABAergic transmission in pallido-pallidal recurrent synapses is under modulation of D_4R, while the D_2R subtype, as known, modulates striato-pallidal projections. Also, as in projection areas, D_4R contributes to control the motor activity differently than D_2R. This study could help to understand the organization of intra-pallidal circuitry.

INTRODUCTION

The Globus pallidus (GP) receives GABA mainly from projections of striatal medium-sized spiny neurons (MSNs) (Parent and Hazrati, 1995a; Parent and Hazrati, 1995b) and the intranuclear collaterals of arkypallidal and prototypic pallidal neurons (Kita and Kitai, 1994; Nambu and Llinas, 1997; Mallet et al., 2012; Abdi et al., 2015). The striato-pallidal fibers constitute the majority of GABAergic terminals in the GP, approximately 65-80% of the total (Smith et al., 1998; Kita, 2007), from which two-thirds come from Enkephaline-positive MSNs that express D_2R and are part of the basal ganglia indirect pathway (Smith et al., 1998). The other terminals are collaterals from Substance P-positive MSNs that express dopamine D_1 receptor (D_1R) (Kawaguchi et al., 1990; Floran et al., 1990). Both afferents terminate mainly on the dendritic shafts of GP neurons (Falls et

al., 1983; Okoyama et al., 1987). Arkypallidal neurons represent about 25% of total GP neurons and send their axons back to the striatum (Str) (Nambu and Llinas, 1997; Mallet et al., 2012; Hernandez et al., 2015). Furthermore, these neurons also send local axon collaterals to the soma and proximal dendrites within GP (Kita and Kitai, 1991; Kita and Kitai, 1994; Bevan et al., 1998; Kita et al., 1999; Kita and Kita, 2001; Abdi et al., 2015). On the other hand, prototypic neurons comprise about 70% of GP projection neurons (Mallet et al., 2012; Hernandez et al., 2015); they send their axons to projection areas such as the Subthalamic nucleus (Sth) (Mallet et al., 2012; Hernandez et al., 2015), the Substantia nigra pars reticulata (SNr) (le Boulch et al., 1991; Parent and Hazrati, 1995b), and the Reticular thalamic nucleus (RTN) (Gandia et al., 1993; Hazrati and Parent, 1991; Kayahara and Nakano, 1998). Moreover, these neurons also send local axon collaterals within GP (Kita and Kitai, 1994; Nambu and Llinas, 1997; Mallet et al., 2012). Pallido-pallidal collaterals constitute 10-20 % of the total GABAergic terminals (Smith et al., 1998; Kita, 2007).

On the other hand, different subtypes of the dopamine D2-like receptors family are expressed predominantly in each population of neurons: D2 receptor subtype (D_2R) is preferentially expressed in enkephalin-positive MSNs (Surmeier et al., 1996), while pallidal neurons express the D4 receptor subtype (D_4R) (Mrzljak et al., 1996; Ariano et al., 1997; Mauger et al., 1998). In this regard, D_2Rs modulate the firing rate of MSNs (Hernandez-Lopez et al., 2000) and the GABA release at striato-pallidal terminals (Floran et al., 1997; Cooper and Stanford, 2001; Caballero-Floran et al., 2016; Jijon-Lorenzo et al., 2018) and striato-striatal collaterals (Guzman et al., 2003). Likewise, D_4Rs modulate the activity of pallidal neurons (Shin et al., 2003; Hernandez et al., 2006) and the GABA release at pallidal projections toward SNr (Acosta-Garcia et al., 2009; Aceves et al., 2011; Cruz-Trujillo et al., 2013), Sth (Floran et al., 2004b), and RTN (Floran et al., 2004a; Gasca-Martinez et al., 2010; Crandall et al., 2010; Govindaiah et al., 2010; Barrientos et al., 2019). However, it is unknown if D_4Rs are present and control the GABA release at pallido-pallidal recurrent collaterals. Also, if by the different proportion of striatal afferent terminals vs. local recurrent terminals, they have a distinct contribution to the control of the GABA release within GP. This second issue is essential since the relative control of total GABA release by one receptor type would determine the motor behavior in a particular pharmacological condition.

Here, we present neurochemical and electrophysiological evidence of the presence of D_4Rs on pallidal recurrent collaterals, whose pharmacological manipulation impacts motor behavior. The functionality of D_4Rs in pallido-pallidal terminals and D_2Rs in striato-pallidal projections was tested by the relative contribution to the total control of GABA release within GP. Finally, the impact of

D_2R and D_4R on motor behavior was evaluated by microinjections of selective antagonists into GP of amphetamine-challenged and not challenged rats.

EXPERIMENTAL PROCEDURES

Animals

All procedures were carried out following the National Institutes of Health Guide for Care and Use of Laboratory Animals and approved by the Institutional Animal Care Committee of the CINVESTAV-IPN. Due to conveniences for technics and the amount of tissue required for experiments, Western blot, [^{3}H] YM-09151-2 D_4R binding, [^{3}H]GABA release, and behavioral observations were done using male Wistar rats age two months (weighing 200-250 gr). They were housed together (five per cage) with water and food available ad libitum and kept under a natural light cycle throughout. Mice (12-14 days postnatal) maintained in similar housing conditions were used for electrophysiological recordings.

Reserpine treatment

For [^{3}H]GABA release experiments in GP slices, rats were pretreated with reserpine (10 mg kg-1, intraperitoneally, i.p.) 18 h before the preparation of slices to avoid the effects of endogenous dopamine, since depolarization with a high K^+ media massively increases endogenous dopamine and activates their receptors (Floran et al., 1997). This treatment produces more than a 90% reduction in dopamine content in the GP (Nava-Asbell et al., 2007).

Lesion of GP with kainic acid

We used a method previously described by le Boulch et al. (1991) and modified by Acosta et al. (2009). In brief, animals were anesthetized with Ketamine/Xylazine (80/10 mg/kg i.p.) and mounted in a stereotaxic apparatus. We injected a kainic acid solution unilaterally (1 µg/µl freshly dissolved in 0.2 M sodium phosphate buffer, pH 7.4) with a Hamilton syringe. A single 0.5 µl injection was used (A = -7.0, L = -3, H = +5.2) employing a peristaltic pump, and at the end of the injection, the needle remained in place for further 5 minutes. Immediately after recovery from anesthesia, rats showed a rotation contralateral to the injected side, as reported previously (le Boulch et al., 1991). After surgery, animals received a single dose of enrofloxacin (2.5 mg/kg) and a daily subcutaneous injection of a 5% glucose solution in saline (1 ml) for five days. Fourteen days after the lesion, animals were sacrificed to dissect the left and right Str, GP, and SNr for D_4R protein western blot in synaptosomes and [^{3}H] YM-09151-2 binding in synaptosomal membranes.

The lesion's extension and selectivity within GP were assessed in rat coronal brain slices stained with NeuN, visualized with fluorescence microscopy, and analyzed for nuclei count with Image J software. In brief, rats were anesthetized with an overdose of pentobarbital (4 mg/kg, i.p.), perfused transcardially with saline Ringer solution followed by 4% paraformaldehyde (PFA) in 0.1 M phosphate buffer (PB), pH 7.4. Brains were dissected and postfixed with 4% PFA for 24 hr at 4°C. After, tissue was dehydrated in 0.1 M PB with 30% sucrose and then embedded in OCT (Miles Inc., Elkhart, IN, USA) and cut into coronal 30 µm sections on a freezing microtome (Leica, Nussloch, Germany). For immunofluorescence, the free-floating sections method was used. Nine slices from bregma 0.7 to -2.4 mm from each rat (3 rats) were selected. Slices were incubated with 0.1% Triton X-100 and 1% serum bovine albumin in 0.1 M PB for 2 hr at room temperature. After complete blocking, sections were incubated with the primary antibody, monoclonal anti-NeuN (Chemicon®) (1:200). The slices were then incubated with the secondary antibody, Alexa Fluor 594 anti-mouse, at room temperature for 3 hours (1:200). Finally, after three washes with PB, slices were mounted in coverslips, washed, and dried. The immunofluorescent cells were viewed by epifluorescence through a 20X objective (numerical aperture [NA]: 0.5) Plan Fluor Lens coupled with a Nikon Eclipse-80i Microscope (Nikon Corp., Tokyo, Japan). Images were obtained and recorded using a Nikon digital sight-DG-Ril camera controlled with the Nikon NIS-Elements AR-3.0-SP7 software (Nikon). Images from three (0.27 mm^2) sections of each slice were obtained, processed for nuclei counting, and analyzed with ImageJ 2.1.0/Java 1.8.0 with the Nucleus Counter plugin. It can be seen in Supplementary figure 1 that kainic acid injection produces a decrement of about 97% of NeuN-stained nuclei in the lesioned GP compared with the non lesioned side. No significant changes in the border of the Str and the posterior regions to GP that include: the ventrolateral thalamic nucleus, ventral anterior thalamic nucleus, reticular thalamic nucleus, ventromedial thalamic nucleus, and ventral-posterolateral thalamic nucleus were observed.

Preparation of brain slices

From mice. The mice were decapitated under anesthesia, and oblique-sagittal slices (300 µM thick), including both the GP and the Str, were cut with a vibroslicer (Campden, Inc.) at an angle of 20° to the midline. The slices were next incubated in oxygenated standard ACSF solution (in mM: NaCl 125, KCl 3, KH2PO4 1.25, NaHCO3 26, MgCl2 1, CaCl2 2.5, D-glucose 10, and equilibrated with 95% O_2 + 5% CO_2, pH 7.4) where they remained for at least one h at room temperature (about 25 °C). From rats. Animals were euthanized, and the brains isolated and immersed in oxygenated ice-cold Artificial Cerebrospinal Fluid (ACSF) solution (composition in mM: NaCl 118.25, KCl 1.75, MgSO4 1, KH2PO4 1.25, NaHCO3 25, CaCl2 2, and D-glucose 10, and bubbled

with 95% O_2 + 5% CO_2, pH 7.4). Coronal brain slices (300 µm thick) were obtained with the vibratome. The GP was microdissected under a stereoscopic microscope. The atlas of Paxinos (1997) was utilized to identify individual nuclei.

Preparation of synaptosomes

Synaptosomal fractions were isolated from Str, GP, and SNr slices from ten rats. The slices were homogenized in buffer (sucrose 0.32 M, HEPES 0.005 M, pH 7.4), and then the homogenates centrifuged at 800 *g* for 10 min. The resulting supernatant was further centrifuged at 20,000 *g* for 20 min. We discarded the supernatant (S1) from this second centrifugation, the pellet (P1) was resuspended and placed in the sucrose 0.8M/HEPES 0.005M buffer (pH 7.4) and newly centrifuged at 20,000 *g* for 20 min. Finally, we discarded the supernatant and employed the new pellet (P2) containing synaptosomes.

Western blotting for D_4R protein

The synaptosomal fraction was incubated with RIPA buffer (sodium orthovanadate 1 mM, sodium pyrophosphate 10 mM, sodium fluoride 100 mM, glycerol 10%, Triton X-100 1%, Tris–HCl 50 mM, NaCl 150 mM, MgCl2 1.5 mM, EGTA 1 mM, SDS 0.1%, and sodium deoxycholate 1%) and a complete set of protease inhibitors (Roche Applied Science, México) for 15 min. Synaptosomal membranes were obtained by sonication of synaptosomes, and then resuspended in sample buffer (Glycerol 50%, Tris-HCl 125 mM, SDS 4%, Bromophenol blue 0.08%, 2-mercaptoethanol 5%) and heated at 100°C for ten min. Protein was quantified by the Bradford method. The samples were resolved by SDS-PAGE, transferred onto PVDF membranes, and blotted for one h at room temperature in Tris-buffered saline containing 0.2% Tween 20 and 5% nonfat powdered milk. Membranes were incubated overnight at 4°C with polyclonal anti dopamine D4 antibody (1:1000) (ab20424; obtained from Abcam Inc. MA, USA). Antibody detection was performed by chemiluminescence (ECL-Plus Amersham) with an HRP-conjugated secondary antibody (1:10,000). Antibody provider test specificity according to the technical note: https://www.abcam.com/drd4-antibody-ab20424.html. The evaluation of band density changes was assessed considering the optic density of the ≈48 kd band from control and lesioned sides divided by the density of their respective actine band and then expressed as percent respect the non-lesioned side.

Binding of D_4R with [^{3}H] YM-09151-2

Binding for D_4Rs in synaptosomal membranes was done according to Marazziti et al. (2009), with slight modifications. The synaptosomal membranes were obtained from GP, Str, and SNr from rats

non-lesioned and lesioned with kainic acid. The tissue was resuspended in buffer Tris-HCl 50mM containing EGTA 1mM (pH 7.4) and homogenized using ten strokes of a handheld homogenizer at 400 rpm. Subsequently, the tissue was centrifuged at 13,000 rpm for 20 min, and the pellet resuspended in D_4R buffer (containing 50mM Tris-HCl, 1mM EDTA, 5mM KCl, 1.5 mM $CaCl_2$, 4mM $MgCl_2$, 120mM NaCl, pH 7.4) for binding assay. One hundred fifteen microliters of GPe and SNr homogenates were incubated with eight increasing concentrations of [^{3}H]-YM-09151-2 (PerkinElmer, Milan, Italy; specific activity: 85.5 Ci/mmol) ranging between 0.015-5 nM, in the presence of raclopride 100 nM at a final volume of 250 microliters. The non-specific binding was carried out by using L-745,870 500nM. The incubation with [^{3}H]-YM-09151-2 was performed for two h at 22°C. The separation of bound and free ligand was carried out by vacuum filtration through GF/C fiber filters (Whatman, UK) pre-soaked in polyethyleneimine (2%) to minimize the non-specific binding to filters. A liquid scintillation counter was employed for counting the radioactivity. Only a concentration of 1 nM of ligand was tested to determine the effect of kainic acid lesions in the number of D_4R binding instead of saturation curves that only were made in normal animals.

[^{3}H]GABA release

[^{3}H]-GABA release was determined with previous methods described in detail by Jijon et al. (2018). In each experiment, Pallidal slices from 8 rats were pooled in a single incubation assay tube and left equilibrating for 30 min in ACSF maintained at 37°C and gassed with O_2/CO_2 (95:5 v/v); then, they were incubated for 30 min in ACSF containing 80 nM [^{3}H]-GABA (95 Ci/mmol). The labeling and perfusion solutions had amino-oxyacetic acid (10 µM) to prevent label degradation by GABA transaminase. At the end of this period, label excess was removed by washing twice with ice-cold ACSF that contained 100 µM nipecotic acid to prevent the recapture of [^{3}H]-GABA. Nipecotic acid was also included in all solutions used in all the following steps of the experiment.

After removing the radioactive solution, slices were transferred to the perfusion chambers and superfused at a rate of 0.5 ml/min. Each chamber (80-µl volume) contained 3-4 slices; 4-5 of the 20 chambers of the superfusion apparatus shape an experimental group. Each chamber was randomly assigned to one experimental group (i.e., the release of each chamber was one replicate). Every experiment has 4-5 experimental groups, as indicated in the graph or results. Experiments were reproduced from 3-8 times as indicated.

After the distribution in the chambers, the slices were superfused with normal ACSF for 30 min before collecting fractions. Basal release of [^{3}H]GABA was measured by collecting four fractions of the superfusate (total volume = 2 ml per fraction) before depolarizing the slices with a solution in

which the [K^+] was raised to 15 mM. The composition of the high K^+ solution was (mM): NaCl 101.25, KCl 13.75, MgSO4 1, KH2PO4 1.25, NaHCO3 25, CaCl2 2, and D-glucose 10, bubbled with 95% O_2 + 5% CO_2, pH 7.4). Six more fractions were collected in the high K^+ medium. All drugs were added to the medium at fraction 2, before changing the superfusion to the high K^+ medium, to explore basal release effects. At the end of the experiment, the slices were collected to determine the total amount of tritium remaining in the tissue, treated with 1 ml of 1N HCl, and allowed to stand for one h before adding the scintillator. [^{3}H]GABA release was initially expressed as a fraction of the total tritium remaining in the tissue. The effect of drugs on the basal release of [^{3}H]GABA was assessed by comparing the fractional release in fraction 2 (immediately before exposure of the tissue to the drug) and fraction four (immediately before exposure to 15 mM of K^+). Changes in K^+-evoked [^{3}H]-GABA release was assessed by comparing the Area Under the appropriate release Curves (AUC) between the first and last fractions collected after the change to high K^+. For each experimental condition, relative areas were expressed as a percentage of control.

Electrophysiological recordings

Recordings of spontaneous inhibitory postsynaptic currents (sIPSC). A single slice from mice was transferred to a recording chamber placed on the stage of an upright microscope (Zeiss Axioscope), where GP neurons were visually identified and sampled (see figure 5). Slices were superfused with ASCF 2 ml/min at room temperature and equilibrated with 95% O_2-5% CO_2 containing (in mM): 126 NaCl, 26 NaHCO3, 3 KCl, 1.25 NaH2PO4, 1.6 CaCl2 , 1.5 MgSO4, and 10 D-glucose, pH 7.45. Patch-clamp recordings were made using borosilicate glass pipettes (impedance 3-6 MΩ) prepared with a micropipette puller (David Kopf 730) and filled with an internal solution containing (in mM): 135 CsCl, 4 NaCl 0.4 GTP, 2 ATP-Mg, 0.5 EGTA Cs, 10 HEPES, and 0.5 $CaCl_2$, pH 7.25. GABA A-receptor-mediated sIPSCs were recorded in whole-cell voltage-clamp mode with a setup integrated by an Axopatch 200B amplifier, an acquisition Digidata 1200 analog-digital apparatus controlled by a Clampex 9.2 package software (Axon Instrument, Foster City, CA), and a digital oscilloscope used to monitor the recording during the experiment. Currents were isolated by incubating slices with 6-cyano-7-nitroquinoxaline-2,3-dione (CNQX, 10µM) and DL-2-amino-phosphonopentanoic acid, (DL-AP-5, 40µM), the NMDA and AMPA receptor antagonists, respectively. Signals were digitized at 20 kHz and low-pass filtered at 2 kHz, with a step pulse of −5mV, we monitored series resistance at the end of each recording. Data were discarded when the series resistance increased by >20%. Sample tracings of these spontaneous currents are shown in Fig 5. Their amplitude ranged from 40 to 100 pA. These discharges were abolished by incubation in

either TTX (1 µM) or bicuculline (10 µM), indicating that they are dependent on spike firing in GABAergic projections (see figure 5).

Evoked GABA A mediated inhibitory postsynaptic currents (eIPSCs). eIPSCs were recorded in whole-cell configuration at a holding potential of -60 mV (after potential junction correction) and isolated with NMDA and AMPA antagonist similar to sIPSCs. Borosilicate pipettes (3-6 MΩ resistance) containing an internal solution of (in mM): 135 K-Gluconate, 4 NaCl, 0.4 GTP, 2 Mg-ATP, 0.5 EGTA, and 10 HEPES, pH 7.25 were employed to characterize electrophysiological properties of GP neurons (figure 5 B and D). In studies where eIPSCs were elicited, the internal solution was the same as for sIPSC. eIPSC was stimulated, giving a train of five pulses every 15 s with a 50 ms interval (20 Hz), using a bipolar platinum/iridium electrode positioned in the Str or within GP. Single rectangular electrical pulses ~10 to 100 mV intensity, 0.5 ms pulse duration was used for stimulation in the Str, and ~1-10 mV, 0.5 ms for stimulation within GP, were delivered through an isolated stimulation unit (DS2; Grass Instruments). Data amplitudes were calculated from the average of more than four trials each minute with Clampex 10 (Molecular Devices), and five-pulse ratios by dividing pulse X/pulse 1 of each condition.

Behavioral observations

Male Wistar rats locally bred weighing 180 to 200 g were anesthetized with ketamine/xylazine (80/10 mg/kg, i.p.). A guide cannula (22 gauge, 14 mm long) was placed in GP of one side for microinjections. The coordinates used were: - 0.4 mm posterior and 3.0 mm lateral to bregma and 4.7 mm from the dura. The cannula was secured in place with dental acrylic glued to the skull and small stainless steel screws; a wire stylet was inserted into the cannula to prevent clogging. Rotational behavior was tested three days after surgery. A single dose of D-amphetamine (1 mg/kg i.p.) or saline was administered. Ten minutes after amphetamine as indicated, the rat was gently restrained, and the stylet was replaced by an injection cannula (30 gauge, 14.5 mm long) connected to a 5 µl Hamilton syringe. Then the animals were returned to the observation chamber. Drugs or vehicle were applied in a volume of 1 µl delivered during 2 min by hand, and the cannula remained in place three additional minutes. The number of turns per minute was registered for every min by two blind independent observators for 40 min more.

Finally, the animals were killed by an overdose of ketamine/xylazine, the brains removed and fixed in 10% of formalin for 24 h. Brain sections (150 µm) were obtained, and injection sites were assessed by the cannula's location on digitized images of the brain slices. These images were superimposed onto schemes of the brain (Paxinos, 1997). Experiments with cannula locations not corresponding to GPe were discarded.

We estimated the spread of microinjected drugs outside of the nucleus by injecting methylene blue into GP to support that the behavioral effect occurs within this nucleus. In a set of experiments, anesthetized rats were injected with a 1 µL of a methylene blue solution 1% (w/v). The animals were sacrificed immediately (0 min), 30 min, or 60 min after the syringe's remotion, and their brains were removed and placed in PBS/PFA 4% for 24 h. Coronal brain slices (100-µm thick) from bregma 0.60 to -1.80 mm containing the GP were obtained with a vibroslicer (Campden Inc., Cambridge, UK) and observed with a stereoscopic microscope. As shown in supplementary figure 2, the dye remains within the pallidal structure even after 60 min, suggesting that drug effects occur by activating GP receptors.

Statistical analysis

All data were analyzed using Graph Pad Software, San Diego CA, USA, version 7.05. Differences in densitometry analysis for D_4R western blotting, Bmax for binding studies, and changes in amplitude or frequency of sIPSC were analyzed with the Wilcoxon matched-pairs signed-rank test. Differences in data from [^{3}H] GABA release, the time course of drug effects on sIPSC, and eIPSC were analyzed with the Kruskal-Wallis test followed by Dunn´s test. Changes in ratios of pulse stimulation of eIPSC were analyzed by the Friedman test followed by Dunn´s test. In the case of comparison of observations between data from different experiments, Man Whitney U-test was performed. In behavioral experiments to obtain an unbiased estimate of Hill number, EC_{50} values and E_{max} concentration-response data for amphetamine-induced turning behavior were fitted by Hill Plot and plotted on a semilog scale. A list of the relative affinities of drugs used in this project to activate D_2R or D_4R is shown in table 1.

Drugs

amino-oxyacetic acid; CNQX, 6-cyano-7-nitroquinoxaline-2,3-dione; DL-AP-5, DL-2-amino5phosphonopentanoic acid; L 741,626, (±)-3-[4-(4-Chlorophenyl)-4-hydroxypiperidinyl]methylindole; L 745,870, 3-[[4-(4-Chlorophenyl)piperazin-1-yl]methyl]-1H-pyrrolo[2,3-b]pyridine hydrochloride; nipecotic acid; PD 168,077, N-[[4-(2-Cyanophenyl)-1-piperazinyl]methyl]-3-methylbenzamide maleate salt; Quinpirole, trans-(–)-(4aR)-4,4a,5,6,7,8,8a,9-Octahydro-5-propyl-1H-pyrazolo[3,4-g]quinoline monohydrochloride; Sulpiride, (S)-5-(Aminosulfonyl)-N-[(1-ethyl-2-pyrrolidinyl)methyl]-2-methoxybenzamide; Sumanirole, (5R)-5,6-Dihydro-5-(methylamino)-4H-imidazo[4,5,1-ij]quinolin-2(1H)-one maleate, all drugs were obtained from Sigma (St. Louis, MO, USA). Radiochemicals: [^{3}H] GABA, aminobutyric acid (GABA) γ-[2,3-3H(N)]-, Specific Activity: 25-40Ci (925GBq-1.48TBq)/mmol, 1mCi (37MBq) and [N-METHYL-^{3}H]

YM-09151-2, cis-N-(1-benzyl-2-methylpyrrolidin-3-yl)-5-chloro-2-methoxy-4-methylaminobenzamide, Specific Activity: 84.4 Ci (3123GBq-1.75TBq)/mmol, 1mCi (9.25 MBq) were purchased from Perkin Elmer.

RESULTS

Location of D_4R in pallido-pallidal collaterals

We evaluated the presence of the D_4R protein in intra-pallidal collateral recurrents. Western blot for D_4R in synaptosomes from the ipsilateral and contralateral sides of GP from rats unilaterally lesioned with kainic acid (le Boulch et al., 1991; Acosta-Garcia et al., 2009) were performed. Also, we measured changes in protein expression in synaptosomes in the projection areas of pallidal neurons: the SNr and the Str. In figure 1A, the presence of D4R protein in synaptosomes of GP at a band of near 48 KDa in the control side (C) can be seen. In the lesioned side (L), a significant decrement in the protein content can be observed, which was confirmed by the densitometry analysis showed in the lower part of the graph (48kDa band percentage of control side; control side 100%, vs. median lesioned side 23%, rank 15-33, *W*=0, p=0.031, n=5 experiments). No D_4R protein changes were observed after intra-pallidal lesion in striatal synaptosomes (Figure 1B, 48kDa band percentage of control side; control side 100%, vs. median denervated side 100%, rank 96-118, W=4, p=0.31, n=5 experiments). As expected, a substantial decrement was also observed in SNr synaptosomes protein (Figure 1C, 48kDa band percentage of control side; control side 100%, vs. median denervated side 34%, rank 22-53, W=15, p=0.031, n=5 experiments).

The membranal expression of D_4R of pallidal, striatal, and nigral synaptosomes in the non-lesioned (control) and lesioned side of unilaterally kainic acid-lesioned animals was determined. We performed saturation binding studies with a non-selective D2-like tritiated ligand [^{3}H] YM-09151-2 with a protocol in which D_2R and D_3R binding were discarded pharmacologically (see methods). In non-lesioned animals, GP presynaptic D_4R has an estimated median B_{max} of 122 fmol/mg protein, rank 98 to 135 and a median Kd of 0.56 nM, rank 0.41 to 0.75 (a representative experiment of five can be seen in figure 2A). In experiments in rats in which one GP had been lesioned with kainic acid, a significant decrement in receptors bound with [^{3}H]YM-09151-2 (1 nM) was found when compared the control and lesioned sides (figure 2D, control side: median bound 84 fmol/mg protein, rank 74-97 vs. median lesioned side 34 fmol/mg protein, ranks 9-36, W=-15, p=0.0313, n=5 experiments). In non-lesioned animals, D_4R in Str has an estimated median B_{max} of 128 fmol/mg protein, rank 114 to 135, and a median Kd of 0.67 nM, rank 0.59-0.78 (a representative experiment of five can be seen in figure 2B), parameters similar to pallidal receptors. However, the pallidal lesion did not modify bound with [^{3}H]YM-09151-2 (figure 2E, control side: median bound

83 fmol/mg protein, rank 68-100 vs. lesioned side median bound 92 fmol/mg protein, ranks 87-99, W=-7, p=0.219, n=5 experiments.). Finally, correspondingly with GP, nigral D_4R had similar sensitivity with a higher expression level measured by a median Bmax of 188 fmol/mg of protein, rank 175-191 and median Kd of 0.65 nM, rank 0.51-0.76 (a representative experiment of five can be seen in figure 2C). Bound of [^{3}H]YM-09151-2 (1 nM) decreased significantly in SNr after pallidal lesion (figure 2F, control side: median bound 150 fmol/mg protein, rank 140-153 vs. median bound lesioned side 13 fmol/mg protein, ranks 8 to 28, W=-15, p=0.031, n=5 experiments). Judging by the Bmax of saturation curves, the estimated number of receptors at nerve terminals was significantly higher in SNr. At the same time, it was similar between GP and Str (median Bmax SNr 188 fmol/mg protein, rank 175-191 vs. median GP 122, rank 98-135, mean rank difference -8.5, p=0.003, and vs. median Str 128, rank 114-135, mean rank difference -6.5, p=0.021 n= five determinations per nucleus, Kruskal-Wallis followed by Dunn´s test). No significant differences were found in Kd (median Kd GP 0.56 nM, rank 0.41-0.75 vs. median Str 0.67, rank 0.59-0.78, mean rank difference -4.6, p=0.103, and vs. median SNr 0.65, rank 0.51-0.76, mean rank difference -3.2, p=0.620 n= five determinations per nucleus). Table 2 summarizes the Bmax and Kd values obtained for the different nuclei and the bound of [^{3}H]YM-09151-2 (1 nM) in control and lesioned sides of kainic acid-lesioned animals.

D_4R has less relative contribution in the total control of GABA release respect to D_2R in GP

Since the motor effects of presynaptic dopamine receptors depend upon their relative expression and their effects on neurotransmitter release (Briones-Lizardi et al., 2019), we studied the relative contribution of D_2R and D_4R in the control of GABA release in GP slices from reserpinized rats. The effect of the D2-like agonist Quinpirole (1µM) on K^+-induced [^{3}H] GABA release is shown in figure 3E, a significant decrement of about 60% was observed (GABA release; median control 100% vs. median Quinpirole 39%, ranks 24-50; mean rank difference 24, ***p<0.001, n=10). The D2-like antagonist Sulpiride (100 nM) prevented all effects of Quinpirole (GABA release; median control 100% vs. median Quinpirole+ Sulpiride 101, ranks 82-114, mean rank difference -2, p=0.70, ns, n=10). In contrast, the blockade of D_4R with its selective antagonist (Patel et al., 1997) L 745,870 (100 nM), prevented partially the Quinpirole effect diminishing it in around 28% (GABA release; median Quinpirole 39%, ranks 24-50 vs. median Quinpirole + L 745,870 69%, ranks 60-75, mean rank difference -10, p=0.05, n=10). These data indicate the control of GABA release by D_2R and D_4R. To establish the sole contribution of D_2R, we performed experiments with slices perfused with the selective D_4R antagonist throughout the experiment (Jijon-Lorenzo et al., 2018). In this condition, D2-like agonist Quinpirole only decreased GABA release in circa of 40% (figure 3F, GABA

release; median control 100% vs. median Quinpirole 64%, ranks 53-71, mean rank difference 10, p=0.0136, n=6). Likewise, Sulpiride prevented all the Quinpirole inhibitory effect without modification of release itself.

As Quinpirole activates all D2-like receptors, we performed experiments with selective D_2R and D_4R agonists to investigate their relative contribution. In figure 3G, is shown the effect of D_2R selective agonist Sumanirole (100 nM, McCall et al., 2005), which inhibits the release circa of 45% (GABA release; median control 100% vs. median Sumanirole 55%, rank 32-59, mean rank difference 15, p=0.0027, n=6), an effect prevented by Sulpiride, but not by the D_4R antagonist L 745,870 (GABA release; median control 100% vs. median Quinpirole + Sulpiride 103%, ranks 74-116, mean rank difference -0.83, p=0.869, ns. GABA release; Sumanirole median 55%, ranks 32-59 vs. median Sumanirole + L745,870 56%, ranks 45-65, mean rank difference -0.33, p=0.947, ns, n=6). Sumanirole was more potent than Quinpirole in the presence of L 745,870 to inhibit GABA release (figure 3F median Quinpirole + L 745,870 64%, ranks 53-71 vs. figure 3G Sumanirole 55%, ranks 32-59, U=5, p=0.368, Mann-Whitney test, n=6 in each group). In contrast, the D_4R selective agonist PD 168,077 (100 nM, Kulagowski et al., 1996), inhibits only circa of 20% GABA release (figure 3H, GABA release median control 100% vs. median PD 168,077 80%, ranks 70-89, mean rank difference 15.17, p=0.0273, n=6), the effect was prevented by the selective D_4R antagonist L 745,870 and by Sulpiride (GABA release; median control 100% vs. median PD 168,077+ L 745,870 99%, ranks 90-128, mean rank difference 0.08, ns; and median control 100% vs. median PD 168,077+Sulpiride 98%, ranks 95-115, mean rank difference -3, ns, n=6 experiments). The magnitude of inhibition produced by PD 168,077 is similar to the difference in the effect of Quinpirole alone compared in the presence of L 745,870 (figure 3E, red bar minus blue bar). Figures 3A-D present the fractional course of typical release experiments of the lower graphs.

D_4R modulates pallidal sIPSC

First, we corroborated that we registered GP neurons correctly. We characterized a set of 17 neurons by their electrophysiological properties. Representative records in current-clamp conditions of the response to different current injections of the two subtypes of neurons that correspond with types A and B in mice previously reported in the literature are shown in supplementary figure 3 (Kita and Kitai, 1991; Stanford and Cooper, 1999; Stanford and Cooper 2000; Shin et al., 2003; Engler et al ., 2006; Bugaysen et al.,2010; Akopian et al., 2016). Type A neurons were characterized by an input resistance of 410±9 MΩ, a firing rate of 8±1 Hz, an action potential duration of 1.8±0.2 ms, a regular firing, and the presence of time- and voltage-dependent “sag” caused by the Ih current and rebound depolarization. Type B neurons were

characterized by an input resistance of 302±9 MΩ, a firing rate of 7±1.4 Hz, an action potential duration of 1.3±0,4 ms, an irregular firing rate, and lack of "sag." We found 11 from 17 characterized neurons (65%) corresponded to type A, and six corresponded to type B. We did not found neurons that putatively correspond to type C. A similar pattern has been identified in the rat GP (Cooper and Stanford, 2000) with comparable proportions. We pooled all neurons' data because we and others (Shin et al., 2003) cannot distinguish between different types of neurons during patch-clamp experiments. The sIPSCs registered were sensitive to TTX and Bicuculline, indicating the GABAergic nature and action potential dependence of currents (Nambu and Llinas, 1994). In supplementary figure 3, we also show representative recordings of sIPSC in non-determined type (A or B) neurons. In the control condition and the presence of CNQX and AP5, it can be seen records whose amplitude ranged from 40 to 100 pA and the frequency from 3.7 to 10.8 Hz. The perfusion of CNQX and AP-5 decreased the frequency but not the mean amplitude. The remaining currents were abolished by pretreatment of TTX (1 µM) and bicuculline (10 µM). Spontaneous activity in GP neurons can be recorded in their somas in a slice preparation. According to Kita and Kitai (1991), it corresponds to action potential mainly from pallidal neurons and, to a lesser extent, from afferents. Thus, it is possible to study both the presynaptic and somatic effects of receptors, in this case, D_4R. Figure 4 shows the effects of Quinpirole (1 µM) on sIPSCs in GP neurons, and its modification by Sulpiride (100 nM) and L 745,870 (100 nM). Quinpirole significantly decreased the inter-event interval but not the amplitude of sIPSC in pallidal neurons in approximately 39% (figures 4D and 4G). The time course of the effect on frequency is shown in figure 4J, which becomes statistically significant respect control period after two minutes of perfusion and with a maximum effect six minutes later. Data for temporal effect on amplitude are not shown because no changes were observed. The cumulative distribution of frequency of inter-event interval and amplitude comparing at minute 5 (before drug perfusion) and minute 15 (ten minutes after initiation of the drug) of a single representative neuron is shown in figures 4D and 4G, respectively. In the same graphs, the percentual change in both parameters from minute 15 respect minute 5 confirmed the decrement in frequency but not in amplitude (figure 4D and 4G, percentage of change in frequency: median control 100% vs. median Quinpirole 60%, ranks 49-80, W=-21, *p=0.0156; percentage of change in amplitude: median control 100% vs. median Quinpirole 95%, ranks 85-114, W=-6, p=0.25 ns, n=6 cells). The lack of a significant effect on sIPSC amplitude was uniform throughout the experiments. Thus, the description of these effects was omitted from the rest of the text. However, they are still shown in the figures.
The effect of Quinpirole on inter-event interval was prevented either by Sulpiride (figure 4E percent of change in frequency: median control Sulpiride 100% vs. median Quinpirole + Sulpiride

98%, ranks 93-131, W=6, p=0.35 ns, n=6) or by the D_4R antagonist L 745,870 administered before D2-like activation (figure 4F, percent of change in frequency: median control L 745,870 100% vs. Quinpirole + L 745,870 102%, ranks 82-108, W=3 p=0.85, t=0.81, n=7). Neither Sulpiride nor L 745,870 modified the amplitude or frequency of IPSC (data not shown). The time course of the effect is shown in figures 4K and 4L. The distribution of frequency of inter-event interval and amplitude compared at minute 5 and minute 15 is depicted in figures 4E, 4F, 4H, and 4I. Figures 4A-4C show representative traces of sIPSC recorded.

D_4R modulates pallidal eIPSC from collaterals but not of striatal afferents

Previous studies indicated that the activation of D_2R located on striatal afferents depresses GABA release (Floran et al., 1997; Cooper and Stanford, 2001), which leads to increased GP neuronal activity (Querejeta et al., 2001). On the other hand, our neurochemical data indicate the presence of D_4R on collateral recurrents of pallidal neurons. Thus, we studied changes of eIPSC by D_2R and D_4R activation stimulating striatal afferents. We placed the stimulation electrode in Str to activate striato-pallidal afferents preferentially, and we put the stimulation electrode within the GP to activate recurrents preferentially. Since both forms of stimulation can evoke IPSC from recurrents and afferents, we discriminated between them by their differences in short term synaptic plasticity (Connelly et al., 2010) by stimulating them with five pulses at 20 Hz, according to Miguelez et al. (2012). We registered a total of 30 neurons whose striatal (28 neurons) or pallidal local stimulation (2 neurons) produced facilitating short term synaptic plasticity, and a total of 42 neurons whose striatal (3 neurons) or pallidal local stimulation (39 neurons) produced depressing short term synaptic plasticity. The effects of D2-like drugs in grouped putative striato-pallidal and pallido-pallidal terminals are summarized in table 3.

The presynaptic action of the D2-like agonist Quinpirole on D_2R was studied at striato-pallidal putative afferents. Quinpirole (1µM) depressed the amplitude of eIPSCs in about 30% (figure 5B and 5E show the time course of the change of 1rst pulse), which becomes significant 1-4 minutes after perfusion, with a maximal effect at minute ten. This effect was associated with a significant increment in synaptic facilitation, as can be seen by the change in the ratio of pulse X/pulse one (figure 5C, median ratio control 1.4, ranks 1-1.62 vs. median ratio in the presence of Quinpirole 1.72, rank 1-2.02, rank-sum difference 7, p=0.0269, n= 13 neurons, 11 from striatal stimulation and two from pallidal stimulation, Friedman test followed by Dunn´s test). The effect of Quinpirole was entirely prevented by the co-perfusion of the D2-like antagonist Sulpiride (100 nM) (figure 5B), which associated with a recovery of the increment in synaptic facilitation judged by the ratio of pulse X/pulse one (figure 5C, median ratio control 1.40, rank 1-1.62 vs. median ratio in the

presence of Quinpirole + Sulpiride 1.37, rank 1 to 1.58, rank-sum difference -2, p=0.527, n= 13 neurons). The inhibitory effect of Quinpirole at putative striato-pallidal terminals was not modified by the D_4R selective antagonist L 745,870, as seen in figure 5E. This effect also corresponds with a lack of modification of the ratio of pulse X/pulse one elicited by Quinpirole (Figure 5F, the median ratio in the presence of Quinpirole 1.89, rank 1 to 2.10 vs. median ratio in the presence of Quinpirole+ L 745,870 1.82, ranks 1 to 2.11, rank sum difference 5, p=0.114, n= 10 neurons all registered by striatal stimulation). Interestingly, not all neurons with facilitatory synaptic plasticity responded to Quinpirole; in a group of seven neurons (about 23%), Quinpirole did not modify eIPSC amplitude and pulse x/pulse one ratio (see table 3).

At putative pallido-pallidal afferents, Quinpirole also inhibited the amplitude of eIPSC (figure 5H), which becomes significant after one minute of perfusion, with a maximal effect at minute ten, similarly to striato-pallidal afferents. This effect produced a decrement in synaptic depression judged by the change in the ratio of pulse X/pulse one (figure 5I, median ratio control 0.87, rank 0.80 to 1 vs. median ratio in the presence of Quinpirole 0.92, rank 0.87 to 1, rank sum difference 8, p=0.011, n=10 neurons, all records obtained by intra-pallidal stimulation). The D_4R selective antagonist L 745,870 (100 nM) reverted the inhibitory effect of Quinpirole on eIPSC amplitude (figure 5H) and recovered the decrement in synaptic depression (Figure 5I, median ratio control 0.87, ranks 0.80-1 vs. median ratio in the presence of Quinpirole + L745,870 0.86, rank 0.77 to 1, rank sum difference 4, p=0.2059; n=ten neurons). In a set of ten neurons, the effect of Quinpirole was also prevented by Sulpiride (not shown in figures, see table 3)

Quinpirole effects were mimicked by the D_4R selective agonist PD 168,077 (100 nM) and also prevented by the co-perfusion of L 745,870, as well as inhibition of eIPSC (figure 5K) and the ratio of pulses (Figure 5L, median ratio control 0.84, rank 0.74-1 vs. median ratio in the presence of PD 168,077 0.91, rank 0.87 to 1, rank sum difference 7, p=0.0269; and vs. median ratio in the presence of PD 168,077 + L 745,870 0.81, ranks 0.75 to 1, rank sum difference 2, p=0.527, n= nine neurons). Importantly, as occurs at putative striato-pallidal neurons, a set of neurons recorded with depressing synaptic plasticity produced by intra-pallidal (10) or striatal (3) stimulation did not respond to Quinpirole, which represents circa of 24% of the total. Representative traces of the eIPSC showing the facilitation or depression of synaptic plasticity of this type of afferents are depicted in figures 5A, 5D, 5G, and 5H (Miguelez et al., 2012).

Pallidal D_4Rs decreased motor activity

Finally, we investigated if presynaptic D_4Rs that control GABA release within GP impact motor behavior and their magnitude compared to D_2Rs. We tested the effect of D_4R antagonist L 745,870

(Kulagowsi et al., 1976; Patel et al., 1997) vs. D_2R antagonist L 741,626 (Kulagowsi et al., 1976; Vangveravong et al., 2010), injected into GP in naïve rats. The effect of intra-pallidal injection of 750 ng of agonists is shown in figure 6E. The D_2R antagonist induces a minimal ipsilateral turning after injection, which was not significantly different from saline (Figure 6F, median of total 40 min turns, saline 7, rank 5-7 vs. median L 741,626 7, ranks 4-10, mean rank difference 0.33, p=0.88, n= 3 rats each group). In contrast, D_4R antagonist produces a modest but significant turning behavior different from saline and L 741,626 (Figure 6F, median of total 40 min turns saline 7, rank 5-7 vs. median L 745,870 47, ranks 42-54, mean rank difference 4.67, p=0.0338, n= 3 rats each group). Then we studied the effect of blockade of both receptors in amphetamine-challenged rats (1mg/kg i.p.) since endogenous dopamine can activate both receptors and, through releasing GABA, can modify the activity of pallidal neurons and motor behavior.

D_4R and D_2R antagonists dose-dependent decreased motor activity manifested by ipsilateral turning behavior (figure 6G and 6H). The effect had more efficacy for D_4R antagonist since E_{max} was higher and statistically different (judged by the confidence interval) from D_2R antagonist (Figure 6I, E_{max} L 745,870, 275 turns/min CI=253 to 312 vs. L 741,626, 129 turns/min CI 120 to 138, n= three rats per dose) and both exhibited similar potency (Figure 6I, EC_{50} L 745,870, 190 ng CI=163 to 243 vs. L 741,626, 186 ng CI 170 to 215, n= three rats per dose, figure 6G). For comparison, the effect of a higher dose of the non-selective D2-like antagonist Sulpiride (1000 ng) is shown compared with the co-administration of 500 ng of L745,870 and 500 ng of L741,626 in a single injection (figure 6J). The ipsilateral turns per minute were nearly similar, indicating the additive effect of antagonists closing similar values to Sulpiride (Figure 6K, median of total 40 min turns Sulpiride 339, ranks 311-378 vs. median L 745,870 + L 741,626 318, ranks 297-335, sum ranks 13,8 U=2, p=0.4, n= 3 rats each group). The approximate location of the cannulas for different drugs injected is shown in figures 6A-6D.

DISCUSSION

Our data indicate the presence and functionality of presynaptic D_4R at pallido-pallidal collaterals that inhibit GABA release similarly to D_2R at striato-pallidal terminals and affect motor behavior. These findings could help understand the pallidal microcircuit and explain the pharmacological effect of D2-like receptor modifications at the GP on motor behavior.

Location of D_4R at pallido-pallidal terminals

The expression of D_4R in GABAergic GP neurons has been reported at the level of protein and mRNA in mice (Mauger et al., 1998), rats (Ariano et al., 1997), and primates (Mrzljak et al., 1996).

This expression is considered lesser than in the prefrontal cortex neurons, but significantly higher than in Str (Ariano et al., 1997). Thus, it is feasible that receptors can be sent to terminals to control release. Here, we found neurochemical evidence for the presence of D_4R in pallido-pallidal collaterals, based on the substantial decrement of protein in pallidal synaptosomes after kainic acid lesion of the GP (figure 1). The fact that a critical decrement also occurs in SNr indicates not only that D_4R is expressed in nigral terminals (Acosta-Garcia et al., 2009), it also demonstrates that the decrement in GP protein occurs in intra-pallidal collaterals from the same neurons that project to SNr, most probably the prototypic pallidal neurons (le Boulch et al., 1991; Parent and Hazrati, 1995b; Mallet et al., 2012). The presence of D_4R in the neuropil of GP has been shown (Rivera et al., 2003), and striatal lesion with ibotenic acid decreases immunoreactivity, suggesting a presynaptic location in striato-pallidal terminals. However, the functionality of these receptors in the control of GABA release has not been found (Cooper and Stanford, 2001; Shin et al., 2003, this paper), and the expression of D_4R by mRNA and protein in Str has been proposed to low (Surmeier et al., 1996; Ariano et al., 1997).

Our binding studies support the presynaptic location of D_4R at pallido-pallidal and pallido-nigral terminals. To our knowledge, this is the first time that receptors are evaluated by binding in SNr and GP terminals. Consistent with protein data, D_4R binding decreased substantially in SNr and GP but not in Str after regional delimitated pallidal kainic acid lesions (figure 2). In all regions, D_4R sensitivity (K_d) was very similar, compatible with literature data concerning Str (Defagot et al., 1997; Marazziti et al., 2009). However, the estimated number of receptors judged by B_{max} is quite different. SNr has the most significant presynaptic D_4R, almost twice as GP or Str (figure 2), which has two possible explanations. One is that the density of receptors is less in GP since not all collaterals express the receptors. We believe that most D_4R is in the prototypic neuron collaterals since the pallidal GABAergic projections to Sth, SNr, and RTN come from these neurons that express the functional D_4R (Floran et al., 2004a; Floran et al., 2004b; Acosta-Garcia et al., 2009; Gasca-Martinez et al., 2010; Aceves et al., 2011; Cruz-Trujillo et al., 2013). In contrast, in the Str, D_4R seems to be mainly located presynaptically in cortical afferents (Vallone et al., 2000; Berger et al., 2001), modulating glutamate release but not GABA (Gonzalez et al., 2012), probably due to the lack of location or functionality in GABAergic pallido-striatal terminals and striatal interneurons. Thus, possibly arkypallidal projections do not express D_4R. Of course, a more rigorous experimental demonstration is required, for example, immunohistochemical studies. The other explanation is that GP neurons traffic and concentrate more D_4R at nigral terminals, and probably in all their projections areas to a more extent, to establish a robust functional control of GABA release.

Regulation of GABA release by intra-pallidal D_4R

The present study revealed that the D_2R agonist Quinpirole depressed both eIPSCs elicited by electrical stimulation at putative striato-pallidal and pallido-pallidal terminals and the sIPSC tetrodotoxin-sensitive GABAergic activity in neurons of the GP. The effect of Quinpirole was prevented by the D_4R selective antagonist L 745,870 (Patel et al., 1997) in eIPSC in pallido-pallidal terminals, and in sIPSC but not in eIPSC at striato-pallidal terminals. Also, the effect of Quinpirole in pallido-pallidal terminals was mimicked by the D_4R selective agonist PD 168,077 (Glasse et al., 1997; Newman et al., 2008).

One would expect that the striatal electrical stimulation would activate both striato-pallidal and pallido-striatal GABAergic fibers whose collaterals terminate in pallidal neurons (Kita and Kitai, 1991; Guzman et al., 2003; Miguelez et al., 2012). However, by striatal stimulation, the majority of responses that we found corresponded to terminals that responded with facilitating synaptic plasticity, i.e., striato-pallidal 70% (21 records), and another 7% (2 records) came from records from intra-pallidal stimulation (see table 3). Striatal stimulation produced a low percentage (23%) of facilitatory records that did not respond to Quinpirole (7 records), which probably represents striato-pallidal projections from collaterals (Kawaguchi et al., 1990) that express D_1R (Floran et al., 1990). On the other hand, striatal stimulation produced a low proportion of records that expresses depressing synaptic responses (3 records), about 7% of the total of records with this type of synaptic plasticity recorded in this study. They did not respond to Quinpirole (see table 3). The differences can be explained because the pallido-pallidal fibers have relatively low-density respect to striato-pallidal fibers (Nambu and Llinas, 1997; Mallet et al., 2012; Hernandez et al., 2015). On the contrary, intra-pallidal stimulation increased the probability of obtaining records of terminals with depression of synaptic plasticity, i.e., pallido-pallidal, about 93% of the total records (see table 3). With this stimulation, 24% did not respond to Quinpirole or PD 168,077, which might represent the collaterals of arkypallidal neurons (Kita and Kitai, 1994; Mallet et al., 2012; Nambu and Llinas, 1997). Thus, the different records with distinct types of synaptic plasticity and response to D2-like agonists represent differences in afferents and collaterals within GP.

In our study, we found that Quinpirole and PD 168,077 affected pallido-pallidal inhibitory inputs by decreasing eIPSC with characteristics of depressive short-term synaptic plasticity. Those agonists reduced eIPSC amplitude and modified the pulse x/pulse one ratio through an L 745,870 sensitive process (figures 5G to 5L). The same effect was observed in pallido-nigral synapses (experiments not shown, Aceves et al., 2011). Change in pulse x/pulse one ratio indicates that the agonist may be acting at the presynaptic site; hence, D_4R control GABA release in collaterals efferents in GP.

The effects of Quinpirole on eIPSC of putative striato-pallidal terminals blocked by Sulpiride but not by L745,870 (figure 5A to 5F) agree with previous observations showing that activation of D_2R but not D_4R depresses GABA release in striato-pallidal terminals (Cooper and Stanford, 2001; Shin et al., 2003) and the inhibition of action potential firing in the GP produced by stimulation of the Str in the anesthetized rat (Querejeta et al., 2001).

Respect the presence of D_4R in striato-pallidal terminals suggested in electron microscopy-based studies (Rivera et al., 2003), possibly these D_4Rs at striato-pallidal terminals are not functional, pharmacologically distinct, or too low to be detected by our methods. In contrast to anatomical data, the decrease of GABA release by D2-like at putative striato-pallidal terminals is not sensitive to D_4R selective antagonist (Cooper et al., 2001; Shin et al., 2003, this paper). Also, GABAergic striatal projection neurons have collaterals within the Str that express D_2R and represent a substantial source of GABA in the Str (Guzman et al., 2003); however, studies evaluating [^{3}H] GABA release in the Str did not show any effect of D_4R selective drugs (Gonzalez et al., 2012). Thus, neurochemical evidence indicates D_4R in striatal neurons, but functional and pharmacological evidence is adverse. We believe that more research should be performed in this sense. A possibility is a low density of this receptor and/or presence in a population of striatal efferents, an extensive sampling of eIPSC in pallidal neurons recorded from stimulation of different regions of the Str could help. Another possibility is a different expression of splicing variants type of D_4R, with different pharmacological sensitivity or strength of signaling (Sanchez-Soto et al., 2019). Thus, exploration with a broad range of selective agonists/antagonists could be useful. Our data, with the reported low expression of D_4R in striatal neurons and the lack of effect of pallidal lesion on the expression of striatal D_4R in synaptosomes, does not support that striato-pallidal terminal have functional D_4Rs.

Miguelez et al. (2012) analyzed pallido-pallidal transmission characterized by depression of short-term plasticity. They found a lack of effect of the D2-like agonist Quinpirole that is contrary to our observations. Several different experimental conditions could be responsible. An alternative explanation for this apparent inconsistency could be the differences in the age and species of studied animals. Sprague–Dawley rats (P30-45) were used for electrophysiological experiments by Miguelez, while we used mice from P12-14. Thus, it is essential to consider that short-term synaptic plasticity is known to change considerably as animals age (Fedchyshyn and Wang, 2005) and probably among species. Other factors could also cause discrepancies. Possibly D_4R-mediated depression of the eIPSC was not seen in these studies because the activity in the scarcer D_4R-bearing pallido-pallidal fibers might have been masked by the responses of the most abundant striato-pallidal fibers bearing D_2R.

On the other hand, it is not established the relationship between the pre and postsynaptic neurons in the recurrent collateral-pallidal neuron adequately (see Hegeman et al., 2016). Thus, it is also possible that the lack of effect of Quinpirole in neurons sampled in the Miguelez study was due to contact from recurrents that do not express D_4R. In this issue, as pointed out (Hegeman et al., 2016), more research in recurrent collateral-type of neuron relationship is necessary, and this can help solve this discrepancy that evidently could help understand the organization of pallidal micro-circuitry. Recent evidence indicates that D_2R on astrocytes modulate striato-pallidal transmission through modulation of GABA transporter (Chazalon et al., 2018), also D_4R seems to be expressed in astrocytes (Miyazaki et al., 2004), thus if a similar modulation of pallido-pallidal transmission occurs, it represents a perspective of this work.

Two ways of GABAergic influences may decrease pallidal neurons spiking, reducing the number of spikes that arrive at the local collateral terminals, one is the striato-pallidal, and another one is the recurrent collaterals (Bugaysen et al., 2013). These influences are characterized by the different firing properties between striatal and pallidal neurons in *in vitro* preparations. The striatal neurons are often silent and may fire at low rates; usually, 3 to 5 spikes/s (Cui et al., 2014) but fire up to 70–100 spikes/s in episodes lasting on the order of seconds associated with specific sensory, motor, or motivational events (Opris et al., 2011). The burst will then produce a profound enhancement of GABA release (Connelly et al., 2010). In contrast, pallidal neurons are highly active. Prototypic neurons fire in a tonic and regular rate in a range of 20–60 Hz, while arkipallidal neurons in ~ 30 Hz *in vitro* and *in vivo* (Abdi et al., 2015). Therefore, the sIPSC responses and eIPSC with synaptic depression mechanisms reflect the activity of pallidal neurons, a specific signature of this synapse. The depressing effects of Quinpirole on tetrodotoxin-sensitive sIPSC in the GP represent a novel finding. GP neurons recorded in slice preparations showed a relatively high rate of sIPSC. GP axons form relatively large boutons with large synapses that terminate mainly on the somata and proximal dendrites (Falls et al., 1983; Okoyama et al., 1987; Kita and Kitai, 1994; Shink and Smith, 1995), which would tend to produce large amplitude sIPSC recorded at the soma. The amplitude of the sIPSC ranged from 10 to over 100 pA with a Cl^- driving force of approximately 50 mV (Ogura and Kita, 2000; Matsui and Kita, 2003, figure 4). Thus, this sIPSC originated from the GP local axon collaterals, and the effect of Quinpirole indicates that activation of D2-like receptors depresses transmission in pallido-pallidal synapses. This evidence also suggests that D_4R most likely mediates the effect because it was antagonized by L 745,870, which has high selectivity for this receptor (Kulagowski et al., 1996; Patel et al., 1997; Glase et al., 1997). In our experiments, D_4R stimulation produced a reduction in the frequency of sIPSC without a change in amplitude. Previously, such a response has been interpreted as evidence for an effect on the presynaptic

terminals (Llano et al., 1991; Ogura and Kita, 2000; Kodirov, 2010; Azad et al., 2014). Although other mechanisms are also conceivable, such as a change in the firing rate of pallidal neurons, the available evidence of dopamine action on pallidal soma concerning GABAergic transmission (Shin et al., 2003) does not support such a mechanism. The authors found that the most significant effect of the D_4R activation in pallidal neurons was the GABAergic transmission blockade by a PKA inhibition dependent mechanism. They also found that striato-pallidal transmission that decreases GABAergic current is not involved in this mechanism because this effect would favor increased pallidal spiking rather than the observed decrease when dopamine was added to the nucleus (Querejeta et al., 2001).

Moreover, this effect would also produce an increment in sIPSC frequency or amplitude, which was not observed in our experiments; thus, our evidence favors a presynaptic action site. The control by D_4R of GABA in the site of action potential´s generation may overlap with the effect of D_4R in the dendritic shafts. Thus, the mechanism of somatic D_4R on the soma of GP neurons should be meticulously examined. Several possible mechanisms could account for D_4R effects on the pallido-pallidal synaptic terminals. These include, among others, an effect on voltage-gated Ca^{2+}-currents reducing their magnitude, as was shown in pallido-nigral terminals (Recillas-Morales et al., 2014). Evidence to select among these specific mechanisms by D_4R in collaterals is not available yet.

Together with the decrease in eIPSC with characteristics of short-term synaptic plasticity, depression and sIPSC frequency induced by Quinpirole and antagonized by L 745,870, are consistent with the conclusion that dopamine acting at presynaptic D_4R reduces the neurotransmitter release at GABAergic terminals within GP, in SNr, and the STN.

Effects of D_2R and D_4R on motor behavior

Intra-pallidal injections of dopamine-related drugs modify motor activity with variable latencies and time-duration but are all related to dopamine receptors activity (Galvan et al., 2001; Kelsey et al., 2009; Caballero-Floran et al., 2016; Avila et al., 2020). In our case, the antagonists produced an asymmetry expressed as turning 2-3 minutes after injection that lasts approximately forty minutes. This length of the effect could be interpreted as an effect of drug diffusion outside the pallidal structure, particularly to the Str. Nevertheless, experiments with injections of methylene blue that has a similar molecular weight as the antagonists used here remain inside GP for one hour, although MW is not the only determinant for the diffusion of the drug in brain tissue (Myers R.D, 1996). Besides, the potency of stimulation of dopamine release by amphetamine can be a factor that influences the duration of the effects. In a previous study, we used challenge with

methamphetamine, a more potent drug, to evoke dopamine mobilization (Caballero-Floran et al., 2016). The duration of pallidly injected drugs lasted near two hours, compared with one hour in the amphetamine challenge used in this study, indicating that the potency of releaser influences the duration of response. Also, amphetamine challenge with doses used in this study induces the firing of striatal neurons within 30 min that return to normal state after 2 hrs (West et al., 1997). We believe that these observations and the fact that no significant turning behavior was observed when drugs were injected in surrounding areas make it feasible to think that the injected antagonist's effect was located in the pallidal structure. In non-challenged rats, only D_4R antagonist L 745,870 induces motor asymmetry expressed as ipsilateral turns (Figure 6E-F), indicating tonic activation of D_4R by endogenous dopamine. In a meeting, we reported that in microdialysis coupled to behavior experiments, intra-nigral perfusion of L 745,870 in normal rats increases GABA release at pallidal projections and promotes motor behavior and turning (Rodriguez et al., 2016). This finding was also compatible with the activation of receptors by endogenous dopamine since the effect was not observed in 6-OH dopamine-lesioned rats. Thus, as indicated in our electrophysiological experiments (Figures 4 and 5), the antagonist perfusion in GP will increase GABA release at presynaptic D_4R. On the contrary, perfusion of D_2R selective antagonist did not modify basal motor activity indicating low o none stimulation by endogenous dopamine to receptors in these conditions. Last, it is similar to D_1R in SNr, since perfusion of D_1R selective antagonist SCH 23390 modifies neither GABA release nor spontaneous motor behavior (Rodriguez-Sanchez et al., 2019).

One of the main differences in the striato-nigral and striato-pallidal neurons that express D_1R and D_2R concerning pallidal neurons that express D4R is the higher spontaneous firing rate of pallidal neurons (Opris et al., 2011; Cui et al., 2014). Probably, dopamine receptors expressed in a high spiking neuron are more sensitive to dopamine or drugs and, consequently, in the modulation of spontaneous motor behavior. In this respect, activation of D_3R by endogenous dopamine regulates glutamate released in the high spiking subthalamic-nigral neurons and motor activity (Rodriguez-Sanchez et al., 2019). A factor that can also contribute to this effect is pallido-pallidal terminals at the soma and initial segment of the pallidal neuron (Kita and Kitai, 1994). This location implies that a minimal change in GABA release could significantly impact neuron firing and, in consequence, motor activity.

In contrast, D_2R located in terminals at dendritic shafts (Falls et al., 1983; Okoyama et al., 1987), requires extensive modification of GABA release at terminals to impact the activity of pallidal output neurons. The goal-directed motor behaviors mediated by D_2R receptors required cortical activation of striatal neurons to trigger motor activity (Albin et al., 1989); this increases firing of

striato-pallidal neuron up to 70 to 100 Hz (Opris et al., 2011) and in this condition, D_2R activation now become evident in motor behavior as proposed in basal ganglia models (Albin et al., 1989). Amphetamine challenge induces significant increments in the firing of striatal neurons related to types of motor behavior (West et al., 1997), similarly as the cortical stimulation.

Blockade of D_4R or D_2R can induce a motor imbalance in amphetamine-treated rats since both increase interstitial GABA in the ipsilateral side of the injection. The pharmacological effect of D_4R and D_2R blockade in a condition in which are activated by an equal amount of dopamine released by amphetamine (figure 6G-6I) indicate a more powerful effect in the control of motor behavior by D_4R, which contrast with the relatively less amount of total GABA controlled by this receptor compared with D_2R (Figure 3). The contrasting less effect of D_4R in the control of GABA release respect D_2R indicates that a selective effect on soma and initial segment of the pallidal neuron can be determinant for a behavioral effect and not only the amount of total GABA release controlled by one receptor. The effect of co-administration of both antagonists is mimicked by the administration of the non-selective antagonist Sulpiride (Figure 6J and 6K), that indicates that manipulation of intra-pallidal D2-like antagonist observed here and in previous reports (Munoz-Arenas et al., 2015; Caballero-Floran et al., 2016) involve both receptors. Thus, the antagonist response differences can be explained by the anatomical targeting of D_2R-regulated striato-pallidal vs. D_4R-regulated pallido-pallidal terminals and their effects on pallidal excitability.

In this regard, systemic injections of D_4R ligands have a weak effect on general motor behavior (Bristow et al., 1997; Millan et al., 1998; Clifford and Waddington, 2000; Nayak and Cassaday, 2003) even though that low doses of drugs bind receptors (Bristow et al., 1997; Patel et al., 1997); thus, D_4R might participate in the low states of motor behavior. The fact that in pathophysiological conditions, such as models of ADHD (Zhang et al., 2001) and Parkinsonism (Erlij et al., 2012), D_4R ligands have a significant effect when administered systemically reinforces this possibility. Nevertheless, the role of other receptors in behavior has been clarified after changing brain activity by previously drug injections (Jiang et al., 1993; Popoli et al., 1994; Florán et al., 2002). Thus, the specific role of D_4R in specific types of behaviors should be studied in more detail.

CONCLUSIONS

Similar to projection areas of prototypic pallidal neurons, GABAergic transmission in pallido-pallidal recurrent synapses is under modulation of D_4R, while the D_2R subtype modulates striato-pallidal projections. As in projection areas, D_4R contributes to control motor behavior that might be different for behavior for D_2R. This study may contribute to understanding the organization of intra-pallidal circuitry.

ACKNOWLEDGMENTS

The funding provided by CINVESTAV supported this work.

DECLARATION OF INTEREST

The authors declare no conflict of interest regarding the publication of this paper.

AUTHOR CONTRIBUTIONS

Designed the study ICR, RNCF, BF; Collected data ICR, RNCF, RJL, JA, SRM, JAAF, BF; Analyzed data ICR, RNCF, JAAF, FPB, GLG, BF; Wrote the manuscript HC and BF.

DATA AVAILABILITY

Data could be obtained upon reasonable request to the corresponding author.

ORCID

Benjamin Florán https://orcid.org/0000-0002-3430-9335

LEGENDS TO FIGURES

Figure 1. D_4R protein is located at pallido-pallidal and pallido-nigral but not in pallido-striatal terminals. A, B, and C are representative western blots of D_4R protein in synaptosomes of GP, Str, and SNr, in the control C and lesioned L sides of rats unilaterally lesioned into the GP with kainic acid. Lower graphs depict the densitometry analysis of five blots expressed as a percentage of D_4R protein with respect to the control side. Data are graphed in Tukey boxes and analyzed by Wilcoxon matched-pairs signed-rank test, W values are 15 in A and C, and 4 in B. *p=0.03, p=0.31 in ns, not significant differences, n=5 experiments.

Figure 2. D_4R binding decreases in pallido-pallidal and pallido-nigral but not in striatal terminals after pallidal kainic acid lesion. A, B, and C show representative saturation curves of [^{3}H]YM-09151-2 in D_4R in synaptosomes of GP, Str, and SNr, respectively. D, E, and F are the specific binding of [^{3}H]YM-09151-2 1nM in synaptosomes of the different nuclei comparing the control and lesioned sides of kainic acid-treated rats. Data are graphed in Tukey boxes and analyzed by

Wilcoxon matched-pairs signed-rank test, W values are -15 in D and F, and -7 in B. *p=0.031, and in ns p=0.219, n=5 experiments.

Figure 3. D_2R control [^{3}H]GABA release to a more extent in GP with respect to D_4R. A, B, C, and D are typical experiments of the fractional course of K^+ induced [^{3}H]GABA release in pallidal slices from the rat; control conditions are in black circles, in the presence of Quinpirole (1μM), the selective D_2R agonist Sumanirole (100 nM) or the selective D_4R agonist PD 168,077 (100 nM). Green and blue circles are different co-administration of antagonists alone or with selective agonists. E, F, G, and H are the change in the relative area under the curve as a percentage of control from upper experiments. Data are graphed in Tukey boxes and analyzed by the Kruskal-Wallis test followed by Dunn's test. In E, ***p<0.001 mean rank difference 24 and **p=0.0066 mean rank difference 14 respect control, # p=0.05 mean rank difference -10, n=ten experiments. In F, *p=0.0136 mean rank difference 10, n= six experiments. In G, **p=0.0027 mean rank difference 15, n= six experiments. In H, *p=0.0273, mean rank difference 15.17, n=six experiments. ns, indicate no significant differences among groups according to Dunn's test.

Figure 4. Quinpirole depressed sIPSC frequency but not amplitude. The inhibitory effects were blocked by L 745,870 and Sulpiride. A, B, and C are sample traces showing spontaneous IPSCs before and during the application of Quinpirole (1 μM), alone (in A), and in the presence of Sulpiride (100 nM, in B) or L 745,870 (100 nM, in C). The cumulative distribution of the inter-event intervals and amplitudes of one typical recording from a neuron are shown respectively in D and G for Quinpirole alone, in E and H in the presence of Sulpiride, and in F and I in the presence of L 745,870. The Kolmogorov–Smirnov test was used to determine the significance of the difference between Quinpirole vs. control or in the presence of Sulpiride or L 745,870. The percentual change of frequency or amplitude in the total amount of neurons recorded is shown in the right graph. Data are graphed in Tukey boxes and analyzed by Wilcoxon matched-pairs signed-rank test, W values are -21 in D and 6 and 3 in E and F respectively, *p=0.0156, and indicated with ns when no significant differences were found, n=6, 6 and 7 neurons recorded in an equal number of experiments. J, K, and L are the time course of the effect of drugs, respectively. The time course is expressed in mean ± standard error, but data analyzed by the Kruskal-Wallis test followed by Dunn's test. KS statistic and p were: 69 and p<0.0001 in J, 7.57, and p=0.94 in K, 23.32, and p=0.0553 in L n= six cells recorded in J and K, and 7 in L. Dunn's test *p<0.05 and ** P<0.01 and ns, not significant differences respect control period.

Figure 5. D_4Rs decrease eIPSCs in putative pallido-pallidal terminals, whereas D_2Rs decrease at putative striato-pallidal terminals grouped independently of recorded by striatal or intra-pallidal stimulation. A, D, G, and J are representative records of eIPSC in GP neurons elicited by striatal or pallidal minimal stimulation of a train of 5 pulses at 20 Hz in control (black trace), D_2R agonist Quinpirole (1μM) or PD 168,077 (100 nM) (red traces), and in the presence of D2-like antagonist Sulpiride (100 nM) or D_4R antagonist L 745,870 (100 nM) (green traces). B, E, H, and K are the time course of the percentage of inhibition of the first pulse compared in the control condition (black points), D2 agonist (red points), and agonist + antagonist drug (green points). The time course was graphed in mean ± standard error, but data analyzed by the Kruskal-Wallis test followed by Dunn's test. KS statistic and p were: 124.2 and $p<0.0001$ in B; 128.3, and $p<0.0001$ in E; 101.1, and $p<0.001$ in H; 106.6, and $p<0.0001$ in K. Dunn´s test: *$p<0.05$, **$p<0.01$ and ***$p<0.001$ and ns, not significant differences respect minute one. C. F, I, and L represent the ratio of the amplitude of pulse x/pulse one, respect to the pulse number in the different experimental conditions. Data are graphed in mean ± SEM and analyzed by Friedman test following Dunn's test. Friedman's statistic and p were: 6.5 and $p=0.0417$ in C, F, and L, 8, and $p=0.0046$ in I. Dunn's test: in C, control vs. + Quinpirole rank sum difference 7, *$p=0.0269$ and control vs. +Sulpiride rank sum difference -2, ns, $p=0.527$. In F control vs. +Quinpirole rank sum difference 7, *$p=0.0269$ and control vs. +L 745,870 rank sum difference 5, ns, $p=0.114$. In I, control vs. +Quinpirole rank sum difference 8, *$p=0.011$ and control vs. +L 745,870 rank sum difference 4, ns, $p=0.2059$. In L, control vs. +PD 168,077 rank sum difference 7, *$p=0.0269$ and control vs. +L 745,870 rank sum difference 2, ns, $p=0.5271$. n= 13 A-C, 10 in D-F, 10 in G-I, and 9 in J-L.

Figure 6. D_2R and D_4R blockade induce ipsilateral turning in amphetamine challenged rats. A, B, C, and D are mixed images of schematic draws and microphotographs of slices. The dots indicate where the cannula's tip was located in each animal of the group, and the pictures are a coronal section from brain slices at the GP of a representative animal of the group. E, G, H, and J are the time courses of turning behavior induced by a single dose (range 50-750 ng) of the selective D_4R antagonist L 745,870 (red circles) or D_2R antagonist L 741,626 (blue circles) Sulpiride (black circles) or a mixed dose of 500 ng of L 745,870 and 500 ng of L 741,626 (mixed red and blue circles), in non-challenged (E) or amphetamine challenged rats (1 mg/kg i.p. G, H, and J). F compares the effect of total ipsilateral turns during the session of drugs of E and K of the J groups. Data graphed in Tukey boxes and analyzed by the Kruskal-Wallis test, followed by Dunn's test in F and by the Mann-Whitney test in K. *$p=0.033$, respect saline or L 741,626 and ns, not significant differences

between groups, n=3 rats per group. I Dose-response curve of the entire session ipsilateral turning of both antagonists from rats of graphs G and H.

LEGENDS TO SUPPLEMENTARY FIGURES

Supplementary figure 1. Location and extension of the kainic acid lesion within GP. A show draws of coronal sections of the rat brain at the level of Striatum, Globus Pallidus, and the posterior region and in squares the site from which microphotographs of slices at the same levels, stained with NeuN, from a rat unilaterally lesioned with kainic acid (0.5 µg) microinjected into the GP. B shows in a draw at the anteroposterior axes, the injection site into de GP, and the approximate levels from bregma from which 30 µM slices were obtained and stained. By fluorescence microscopy, three campuses were selected for Image J analysis as shown in A. C, comparison of the count of NeuN positive nucleus from 3 slices, of three campuses of three lesioned animals, at the level of the striatum (black filled-open bar), Globus Pallidus (red filled-open bars), and the posterior area (green filled-open bar), graphed in mean ± SEM, ***p<0.001, student t-test.

Supplementary figure 2. Microphotographs of brain slices in which the spread of 1 µL of methylene blue solution 1% (w/v) microinjected into GP of normal rats and sacrificed immediately 30 and 60 minutes after injections were determined. One 100 µM thick coronal slices from bregma 0.60 to -1.80 mm and visualized by stereoscopic microscopy. As can be observed, methylene blue does not diffuse out the pallidal structure indicated with a dotted line even after one hour of injection.

Supplementary figure 3. Types of GP neurons and characteristics of sIPSC recorded. A and B show the typical current-voltage relationship of the two main types of pallidal neurons recorded within GP. Record of A corresponds to a type “A” reported by Cooper and Stanford (2001) with its characteristic “sag” (11 from 17 neurons). B record corresponds to type “B” (6 from 17 neurons). No records of type C neuron were obtained in our sampling. C and D are representative traces of sIPSC from a different set of neurons, recorded before and after the treatment with CNQX (10 µM) and AP5 (40 µM), to block glutamatergic currents. In C, Bicuculline (10 µM) was added to show the GABAergic nature of the recordings, whereas, in D, TTX (1µM) was added to show the action potential dependence.

REFERENCES

Abdi A, Mallet N, Mohamed FY, Sharott A, Dodson PD, Nakamura KC, Suri S, Avery SV, Larvin JT, Garas FN, Garas SN, Vinciati F, Morin S, Bezard E, Baufreton J, Magill PJ. 2015. Prototypic and arkypallidal neurons in the dopamine-intact external globus pallidus. The Journal of neuroscience : the official journal of the Society for Neuroscience 35(17):6667-6688.

Aceves JJ, Rueda-Orozco PE, Hernandez-Martinez R, Galarraga E, Bargas J. 2011. Bidirectional plasticity in striatonigral synapses: a switch to balance direct and indirect basal ganglia pathways. Learn Mem 18(12):764-773.

Acosta-Garcia J, Hernandez-Chan N, Paz-Bermudez F, Sierra A, Erlij D, Aceves J, Floran B. 2009. D4 and D1 dopamine receptors modulate [3H] GABA release in the substantia nigra pars reticulata of the rat. Neuropharmacology 57(7-8):725-730.

Akopian G, Barry J, Cepeda C, Levine, MS. 2016. Altered membrane properties and firing patterns of external globus pallidus neurons in the R6/2 mouse model of Huntington's disease. Journal of Neuroscience Research 94(12): 1400-1410.

Albin RL, Young AB, Penney JB. 1989. The functional anatomy of basal ganglia disorders. Trends in neurosciences 12(10):366-375.

Ariano MA, Wang J, Noblett KL, Larson ER, Sibley DR. 1997. Cellular distribution of the rat D4 dopamine receptor protein in the CNS using anti-receptor antisera. Brain research 752(1-2):26-34.

Avila G, Picazo O, Chuc-Meza E, García-Ramirez M. 2020. Reduction of dopaminergic transmission in the globus pallidus increases anxiety-like behavior without altering motor activity. Behavioural Brain Research, 112589.

Azad C EM, Mariscano G, Lutz B, Zieglgansberger W, Rammes G. 2014. Activation of the Cannabinoid Receptor Type 1 Decreases Glutamatergic and GABA Synaptic Transmission in the Lateral Amygdala of the mouse. Learning & Memory 10:116-128.

Barrientos R, Alatorre A, Martinez-Escudero J, Garcia-Ramirez M, Oviedo-Chavez A, Delgado A, Querejeta E. 2019. Effects of local activation and blockade of dopamine D4 receptors in the spiking activity of the reticular thalamic nucleus in normal and in ipsilateral dopamine-depleted rats. Brain research 1712:34-46.

Berger MA, Defagot MC, Villar MJ, Antonelli MC. 2001. D4 dopamine and metabotropic glutamate receptors in cerebral cortex and striatum in rat brain. Neurochemical research 26(4):345-352.

Bevan MD, Booth PA, Eaton SA, Bolam JP. 1998. Selective innervation of neostriatal interneurons by a subclass of neuron in the globus pallidus of the rat. The Journal of neuroscience : the official journal of the Society for Neuroscience 18(22):9438-9452.

Briones-Lizardi LJ, Cortes H, Avalos-Fuentes JA, Paz-Bermudez FJ, Aceves J, Erlij D, Floran B. 2019. Presynaptic control of [(3)H]-glutamate release by dopamine receptor subtypes in the rat substantia nigra. Central role of D1 and D3 receptors. Neuroscience 406:563-579.

Bristow LJ, Collinson N, Cook GP, Curtis N, Freedman SB, Kulagowski JJ, Leeson PD, Patel S, Ragan CI, Ridgill M, Saywell KL, Tricklebank MD. 1997. L-745,870, a subtype selective dopamine D4 receptor antagonist, does not exhibit a neuroleptic-like profile in rodent behavioral tests. J Pharmacol Exp Ther 283(3):1256-1263.

Bugaysen J, Bar-Gad I, Korngreen A. 2013. Continuous modulation of action potential firing by a unitary GABAergic connection in the globus pallidus in vitro. The Journal of neuroscience : the official journal of the Society for Neuroscience 33(31):12805-12809.

Caballero-Floran RN, Conde-Rojas I, Oviedo Chavez A, Cortes-Calleja H, Lopez-Santiago LF, Isom LL, Aceves J, Erlij D, Floran B. 2016. Cannabinoid-induced depression of synaptic transmission is switched to stimulation when dopaminergic tone is increased in the globus pallidus of the rodent. Neuropharmacology 110(Pt A):407-418.

Chazalon M, Paredes-Rodriguez E, Morin S, Martinez A, Cristóvão-Ferreira S, Vazuqez S, ... Baufreton J. 2018. GAT-3 dysfunction generates tonic inhibition in external globus pallidus neurons in parkinsonian rodents. Cell reports 23(6): 1678-1690.

Clifford JJ, Waddington JL. 2000. Topographically based search for an "Ethogram" among a series of novel D(4) dopamine receptor agonists and antagonists. Neuropsychopharmacology 22(5):538-544.

Connelly WM, Schulz JM, Lees G, Reynolds JN. 2010. Differential short-term plasticity at convergent inhibitory synapses to the substantia nigra pars reticulata. The Journal of neuroscience : the official journal of the Society for Neuroscience 30(44):14854-14861.

Cooper AJ, Stanford IM. 2000. Electrophysiological and morphological characteristics of three subtypes of rat globus pallidus neurone in vitro. The Journal of physiology 527 Pt 2:291-304.

Cooper AJ, Stanford IM. 2001. Dopamine D2 receptor mediated presynaptic inhibition of striatopallidal GABA(A) IPSCs in vitro. Neuropharmacology 41(1):62-71.

Crandall SR, Govindaiah G, Cox CL. 2010. Low-threshold Ca2+ current amplifies distal dendritic signaling in thalamic reticular neurons. The Journal of neuroscience : the official journal of the Society for Neuroscience 30(46):15419-15429.

Cruz-Trujillo R, Avalos-Fuentes A, Rangel-Barajas C, Paz-Bermudez F, Sierra A, Escartin-Perez E, Aceves J, Erlij D, Floran B. 2013. D3 dopamine receptors interact with dopamine D1 but not D4 receptors in the GABAergic terminals of the SNr of the rat. Neuropharmacology 67:370-378.

Cui G, Jun SB, Jin X, Luo G, Pham MD, Lovinger DM, Vogel SS, Costa RM. 2014. Deep brain optical measurements of cell type-specific neural activity in behaving mice. Nat Protoc 9(6):1213-1228.

Dayne Mayfield R, Larson G, Orona RA, Zahniser NR. 1996. Opposing actions of adenosine A2a and dopamine D2 receptor activation on GABA release in the basal ganglia: evidence for an A2a/D2 receptor interaction in globus pallidus. Synapse 22(2):132-138.

Defagot MC, Malchiodi EL, Villar MJ, Antonelli MC. 1997. Distribution of D4 dopamine receptor in rat brain with sequence-specific antibodies. Brain Res Mol Brain Res 45(1):1-12.

DeLong MR. 1990. Primate models of movement disorders of basal ganglia origin. Trends in neurosciences 13(7):281-285.

Engler B, Freiman I, Urbanski M, Szabo B. 2006. Effects of exogenous and endogenous cannabinoids on GABAergic neurotransmission between the Caudate-Putamen and the Globus Pallidus of the mouse. J Pharmac Exp Ther 316:608-617.

Erlij D, Acosta-Garcia J, Rojas-Marquez M, Gonzalez-Hernandez B, Escartin-Perez E, Aceves J, Floran B. 2012. Dopamine D4 receptor stimulation in GABAergic projections of the globus pallidus to the reticular thalamic nucleus and the substantia nigra reticulata of the rat decreases locomotor activity. Neuropharmacology 62(2):1111-1118.

Falls WM, Park MR, Kitai ST. 1983. An intracellular HRP study of the rat globus pallidus. II. Fine structural characteristics and synaptic connections of medially located large GP neurons. The Journal of comparative neurology 221(2):229-245.

Fedchyshyn MJ, Wang LY. 2005. Developmental transformation of the release modality at the calyx of Held synapse. The Journal of neuroscience : the official journal of the Society for Neuroscience 25(16):4131-4140.

Floran B, Aceves J, Sierra A, Martinez-Fong D. 1990. Activation of D<inf>1</inf> dopamine receptors stimulates the release of GABA in the basal ganglia of the rat. Neuroscience letters 116(1-2):136-140.

Florán B, Barajas C, Florán L, Erlij D, Aceves J. 2002. Adenosine A1 receptors control dopamine D1-dependent [3H]GABA release in slices of substantia nigra pars reticulata and motor behavior in the rat. Neuroscience 115(3):743-751.

Floran B, Floran L, Erlij D, Aceves J. 2004a. Activation of dopamine D4 receptors modulates [3H]GABA release in slices of the rat thalamic reticular nucleus. Neuropharmacology 46(4):497-503.

Floran B, Floran L, Erlij D, Aceves J. 2004b. Dopamine D4 receptors inhibit depolarization-induced [3H]GABA release in the rat subthalamic nucleus. European journal of pharmacology 498(1-3):97-102.

Floran B, Floran L, Sierra A, Aceves J. 1997. D2 receptor-mediated inhibition of GABA release by endogenous dopamine in the rat globus pallidus. Neuroscience letters 237(1):1-4.

Gandia JA, De Las Heras S, Garcia M, Gimenez-Amaya JM. 1993. Afferent projections to the reticular thalamic nucleus from the globus pallidus and the substantia nigra in the rat. Brain Res Bull 32(4):351-358.

Gasca-Martinez D, Hernandez A, Sierra A, Valdiosera R, Anaya-Martinez V, Floran B, Erlij D, Aceves J. 2010. Dopamine inhibits GABA transmission from the globus pallidus to the thalamic reticular nucleus via presynaptic D4 receptors. Neuroscience 169(4):1672-1681.

Glase SA, Akunne HC, Georgic LM, Heffner TG, MacKenzie RG, Manley PJ, Pugsley TA, Wise LD. 1997. Substituted [(4-phenylpiperazinyl)-methyl]benzamides: selective dopamine D4 agonists. Journal of medicinal chemistry 40(12):1771-1772.

Gonzalez S, Rangel-Barajas C, Peper M, Lorenzo R, Moreno E, Ciruela F, Borycz J, Ortiz J, Lluis C, Franco R, McCormick PJ, Volkow ND, Rubinstein M, Floran B, Ferre S. 2012. Dopamine D4 receptor, but not the ADHD-associated D4.7 variant, forms functional heteromers with the dopamine D2S receptor in the brain. Molecular psychiatry 17(6):650-662.

Govindaiah G, Wang T, Gillette MU, Crandall SR, Cox CL. 2010. Regulation of inhibitory synapses by presynaptic D(4) dopamine receptors in thalamus. Journal of neurophysiology 104(5):2757-2765.

Guzman JN, Hernandez A, Galarraga E, Tapia D, Laville A, Vergara R, Aceves J, Bargas J. 2003. Dopaminergic modulation of axon collaterals interconnecting spiny neurons of the rat striatum. The Journal of neuroscience : the official journal of the Society for Neuroscience 23(26):8931-8940.

Hauber W, Lutz S. 1999. Dopamine D1 or D2 receptor blockade in the globus pallidus produces akinesia in the rat. Behav Brain Res 106(1-2):143-150.

Hazrati LN, Parent A. 1991. Projection from the external pallidum to the reticular thalamic nucleus in the squirrel monkey. Brain research 550(1):142-146.

Hegeman DJ, Hong ES, Hernandez VM, Chan CS. 2016. The external globus pallidus: progress and perspectives. The European journal of neuroscience 43(10):1239-1265.

Hernandez-Lopez S, Tkatch T, Perez-Garci E, Galarraga E, Bargas J, Hamm H, Surmeier DJ. 2000. D2 dopamine receptors in striatal medium spiny neurons reduce L-type Ca2+ currents and excitability via a novel PLC[beta]1-IP3-calcineurin-signaling cascade. The Journal of neuroscience : the official journal of the Society for Neuroscience 20(24):8987-8995.

Hernandez A, Ibanez-Sandoval O, Sierra A, Valdiosera R, Tapia D, Anaya V, Galarraga E, Bargas J, Aceves J. 2006. Control of the subthalamic innervation of the rat globus pallidus by D2/3 and D4 dopamine receptors. Journal of neurophysiology 96(6):2877-2888.

Hernandez VM, Hegeman DJ, Cui Q, Kelver DA, Fiske MP, Glajch KE, Pitt JE, Huang TY, Justice NJ, Chan CS. 2015. Parvalbumin+ Neurons and Npas1+ Neurons Are Distinct Neuron Classes in the Mouse External Globus Pallidus. The Journal of neuroscience : the official journal of the Society for Neuroscience 35(34):11830-11847.

Jiang H, Jackson-Lewis V, Muthane U, Dollison A, Ferreira M, Espinosa A, Parsons B, Przedborski S. 1993. Adenosine receptor antagonists potentiate dopamine receptor agonist-induced rotational behavior in 6-hydroxydopamine-lesioned rats. Brain research 613(2):347-351.

Jijon-Lorenzo R, Caballero-Floran IH, Recillas-Morales S, Cortes H, Avalos-Fuentes JA, Paz-Bermudez FJ, Erlij D, Floran B. 2018. Presynaptic Dopamine D2 Receptors Modulate [(3)H]GABA Release at StriatoPallidal Terminals via Activation of PLC-->IP3-->Calcineurin and Inhibition of AC-->cAMP-->PKA Signaling Cascades. Neuroscience 372:74-86.

Kawaguchi Y, Wilson CJ, Emson PC. 1990. Projection subtypes of rat neostriatal matrix cells revealed by intracellular injection of biocytin. The Journal of neuroscience : the official journal of the Society for Neuroscience 10(10):3421-3438.

Kayahara T, Nakano K. 1998. The globus pallidus sends axons to the thalamic reticular nucleus neurons projecting to the centromedian nucleus of the thalamus: a light and electron microscope study in the cat. Brain Res Bull 45(6):623-630.

Kelsey JE, Langelier NA, Oriel BS, Reedy C. 2009. The effects of systemic, intrastriatal, and intrapallidal injections of caffeine and systemic injections of A2A and A1 antagonists on forepaw stepping in the unilateral 6-OHDA-lesioned rat. Psychopharmacology 201(4): 529-539.

Kita H. 2007. Globus pallidus external segment. Progress in brain research 160:111-133.

Kita H, Kita T. 2001. Number, origins, and chemical types of rat pallidostriatal projection neurons. The Journal of comparative neurology 437(4):438-448.

Kita H, Kitai ST. 1991. Intracellular study of rat globus pallidus neurons: membrane properties and responses to neostriatal, subthalamic and nigral stimulation. Brain research 564(2):296-305.

Kita H, Kitai ST. 1994. The morphology of globus pallidus projection neurons in the rat: an intracellular staining study. Brain research 636(2):308-319.

Kita H, Tokuno H, Nambu A. 1999. Monkey globus pallidus external segment neurons projecting to the neostriatum. Neuroreport 10(7):1467-1472.

Kodirov SA, Jasiewicz J, Amirmahani P, Psyrakis D, Bonni K, Wehrmeister M, Lutz B. 2010. Endogenous cannabinoids trigger the depolarization-induced suppression of excitation in the lateral amygdala. Learn Mem 17(1):43-49.

Kulagowski JJ, Broughton HB, Curtis NR, Mawer IM, Ridgill MP, Baker R, Emms F, Freedman SB, Marwood R, Patel S, Patel S, Ragan CI, Leeson PD. 1996. 3-((4-(4-Chlorophenyl)piperazin-1-yl)-methyl)-1H-pyrrolo-2,3-b-pyridine: an antagonist with high affinity and selectivity for the human dopamine D4 receptor. Journal of medicinal chemistry 39(10):1941-1942.

le Boulch NL, Truong-Ngoc NA, Gauchy C, Besson MJ. 1991. In vivo release of newly synthesized [3H]GABA in the substantia nigra of the rat: relative contribution of GABA striato-pallido-nigral afferents and nigral GABA neurons. Brain research 559(2):200-210.

Llano I, Leresche N, Marty A. 1991. Calcium entry increases the sensitivity of cerebellar Purkinje cells to applied GABA and decreases inhibitory synaptic currents. Neuron 6(4):565-574.

Mallet N, Micklem BR, Henny P, Brown MT, Williams C, Bolam JP, Nakamura KC, Magill PJ. 2012. Dichotomous organization of the external globus pallidus. Neuron 74(6):1075-1086.

Marazziti D, Baroni S, Masala I, Giannaccini G, Betti L, Palego L, Catena Dell'Osso M, Consoli G, Castagna M, Lucacchini A. 2009. [(3)H]-YM-09151-2 binding sites in human brain postmortem. Neurochem Int 55(7):643-647.

Matsui T, Kita H. 2003. Activation of group III metabotropic glutamate receptors presynaptically reduces both GABAergic and glutamatergic transmission in the rat globus pallidus. Neuroscience 122(3):727-737.

Mauger C, Sivan B, Brockhaus M, Fuchs S, Civelli O, Monsma F, Jr. 1998. Development and characterization of antibodies directed against the mouse D4 dopamine receptor. The European journal of neuroscience 10(2):529-537.

McCall RB, Lookingland KJ, Bedard PJ, Huff RM. 2005. Sumanirole, a highly dopamine D2-selective receptor agonist: in vitro and in vivo pharmacological characterization and efficacy in animal models of Parkinson's disease. J Pharmacol Exp Ther 314(3):1248-1256.

Miguelez C, Morin S, Martinez A, Goillandeau M, Bezard E, Bioulac B, Baufreton J. 2012. Altered pallido-pallidal synaptic transmission leads to aberrant firing of globus pallidus neurons in a rat model of Parkinson's disease. The Journal of physiology 590(22):5861-5875.

Millan MJ, Newman-Tancredi A, Brocco M, Gobert A, Lejeune F, Audinot V, Rivet JM, Schreiber R, Dekeyne A, Spedding M, Nicolas JP, Peglion JL. 1998. S 18126 ([2-[4-(2,3-dihydrobenzo[1,4]dioxin-6-yl)piperazin-1-yl methyl]indan-2-yl]), a potent, selective and competitive antagonist at dopamine D4 receptors: an in vitro and in vivo comparison with L 745,870 (3-(4-[4-chlorophenyl]piperazin-1-yl)methyl-1H-pyrrolo[2, 3b]pyridine) and raclopride. J Pharmacol Exp Ther 287(1):167-186.

Miyazaki I, Asanuma M, Diaz-Corrales FJ, Miyoshi K, Ogawa N. 2004. Direct evidence for expression of dopamine receptors in astrocytes from basal ganglia. Brain research 1029(1): 120-123.

Mrzljak L, Bergson C, Pappy M, Huff R, Levenson R, Goldman-Rakic PS. 1996. Localization of dopamine D4 receptors in GABAergic neurons of the primate brain. Nature 381(6579):245-248.

Munoz-Arenas G, Paz-Bermudez F, Baez-Cordero A, Caballero-Floran R, Gonzalez-Hernandez B, Floran B, Limon ID. 2015. Cannabinoid CB1 receptors activation and coactivation with D2 receptors modulate GABAergic neurotransmission in the globus pallidus and increase motor asymmetry. Synapse 69(3):103-114.

Myers RD. 1966. Injection of solutions into cerebral tissue: relation between volume and diffusion. Physiology & Behavior 1(2): 171-IN9.

Nambu A, Llinas R. 1994. Electrophysiology of globus pallidus neurons in vitro. Journal of neurophysiology 72(3):1127-1139.

Nambu A, Llinas R. 1997. Morphology of globus pallidus neurons: its correlation with electrophysiology in guinea pig brain slices. The Journal of comparative neurology 377(1):85-94.

Nava-Asbell C, Paz-Bermudez F, Erlij D, Aceves J, Floran B. 2007. GABA(B) receptor activation inhibits dopamine D1 receptor-mediated facilitation of [(3)H]GABA release in substantia nigra pars reticulata. Neuropharmacology 53(5):631-637.

Nayak S, Cassaday HJ. 2003. The novel dopamine D4 receptor agonist (PD 168,077 maleate): doses with different effects on locomotor activity are without effect in classical conditioning. Prog Neuropsychopharmacol Biol Psychiatry 27(3):441-449.

Ogura M, Kita H. 2000. Dynorphin exerts both postsynaptic and presynaptic effects in the Globus pallidus of the rat. Journal of neurophysiology 83(6):3366-3376.

Okoyama S, Nakamura Y, Moriizumi T, Kitao Y. 1987. Electron microscopic analysis of the synaptic organization of the globus pallidus in the cat. The Journal of comparative neurology 265(3):323-331.

Opris I, Lebedev M, Nelson RJ. 2011. Motor Planning under Unpredictable Reward: Modulations of Movement Vigor and Primate Striatum Activity. Front Neurosci 5:61.

Parent A, Hazrati LN. 1995a. Functional anatomy of the basal ganglia. I. The cortico-basal ganglia-thalamo-cortical loop. Brain Res Brain Res Rev 20(1):91-127.

Parent A, Hazrati LN. 1995b. Functional anatomy of the basal ganglia. II. The place of subthalamic nucleus and external pallidum in basal ganglia circuitry. Brain Res Brain Res Rev 20(1):128-154.

Patel S, Freedman S, Chapman KL, Emms F, Fletcher AE, Knowles M, Marwood R, McAllister G, Myers J, Curtis N, Kulagowski JJ, Leeson PD, Ridgill M, Graham M, Matheson S, Rathbone D, Watt AP, Bristow LJ, Rupniak NM, Baskin E, Lynch JJ, Ragan CI. 1997. Biological profile of L-745,870, a selective antagonist with high affinity for the dopamine D4 receptor. J Pharmacol Exp Ther 283(2):636-647.

Paxinos, G.W.C., 1997. The rat brain in stereotaxic coordinates. Academic Press. San Diego CA

Pillai G, Brown NA, McAllister G, Milligan G, Seabrook GR. 1998. Human D2 and D4 dopamine receptors couple through betagamma G-protein subunits to inwardly rectifying K+ channels (GIRK1) in a Xenopus oocyte expression system: selective antagonism by L-741,626 and L-745,870 respectively. Neuropharmacology 37(8):983-987.

Popoli P, Pezzola A, de Carolis AS. 1994. Modulation of striatal adenosine A1 and A2 receptors induces rotational behaviour in response to dopaminergic stimulation in intact rats. European journal of pharmacology 257(1-2):21-25.

Querejeta E, Delgado A, Valdiosera R, Erlij D, Aceves J. 2001. Intrapallidal D2 dopamine receptors control globus pallidus neuron activity in the rat. Neuroscience letters 300(2):79-82.

Recillas-Morales S, Sanchez-Vega L, Ochoa-Sanchez N, Caballero-Floran I, Paz-Bermudez F, Silva I, Aceves J, Erlij D, Floran B. 2014. L-type Ca(2)(+) channel activity determines modulation of GABA release by dopamine in the substantia nigra reticulata and the globus pallidus of the rat. Neuroscience 256:292-301.

Rivera A, Trias S, Penafiel A, Angel Narvaez J, Diaz-Cabiale Z, Moratalla R, de la Calle A. 2003. Expression of D4 dopamine receptors in striatonigral and striatopallidal neurons in the rat striatum. Brain research 989(1):35-41.

Rodríguez M, Escartín-Pérez E, Loya-López S, Erlij D, Floran B. 2016. Motor effects of nigral D4 receptors in normal and hemiparkinsonian rats. Soc Neursc Abstr 498.16

Rodríguez-Sánchez M, Escartín-Pérez RE, Leyva-Gómez G, Avalos-Fuentes JA, Paz-Bermúdez FJ, Loya-López SI, ... Florán B. 2019. Blockade of Intranigral and Systemic D3 Receptors

Stimulates Motor Activity in the Rat Promoting a Reciprocal Interaction among Glutamate, Dopamine, and GABA. Biomolecules 9(10): 511.

Sánchez-Soto M, Yano H, Cai NS, Casadó-Anguera V, Moreno E, Casadó V, Ferré S. 2019. Revisiting the Functional Role of Dopamine D 4 Receptor Gene Polymorphisms: Heteromerization-Dependent Gain of Function of the D 4.7 Receptor Variant. Molecular neurobiology 56(7): 4778-4785.

Shin RM, Masuda M, Miura M, Sano H, Shirasawa T, Song WJ, Kobayashi K, Aosaki T. 2003. Dopamine D4 receptor-induced postsynaptic inhibition of GABAergic currents in mouse globus pallidus neurons. The Journal of neuroscience : the official journal of the Society for Neuroscience 23(37):11662-11672.

Shink E, Smith Y. 1995. Differential synaptic innervation of neurons in the internal and external segments of the globus pallidus by the GABA- and glutamate-containing terminals in the squirrel monkey. The Journal of comparative neurology 358(1):119-141.

Smith Y, Bevan MD, Shink E, Bolam JP. 1998. Microcircuitry of the direct and indirect pathways of the basal ganglia. Neuroscience 86(2):353-387.

Stanford IM, Cooper AJ. 1999. Presynaptic mu and delta opioid receptor modulation of GABAA IPSCs in the rat globus pallidus in vitro. The Journal of neuroscience : the official journal of the Society for Neuroscience 19(12):4796-4803.

Surmeier DJ, Song WJ, Yan Z. 1996. Coordinated expression of dopamine receptors in neostriatal medium spiny neurons. The Journal of neuroscience : the official journal of the Society for Neuroscience 16(20):6579-6591.

Svingos AL, Periasamy S, Pickel VM. 2000. Presynaptic dopamine D(4) receptor localization in the rat nucleus accumbens shell. Synapse 36(3):222-232.

Vallone D, Picetti R, Borrelli E. 2000. Structure and function of dopamine receptors. Neurosci Biobehav Rev 24(1):125-132.

Vangveravong S, Taylor M, Xu J, Cui J, Calvin W, Babic S, Luedtke RR, Mach RH. 2010. Synthesis and characterization of selective dopamine D2 receptor antagonists. 2. Azaindole, benzofuran, and benzothiophene analogs of L-741,626. Bioorg Med Chem 18(14):5291-5300.

West MO, Peoples LL, Michael A J, Chapin JK. Woodward DJ. 1997. Low-dose amphetamine elevates movement-related firing of rat striatal neurons. Brain research 745(1-2): 331-335.

Zhang K, Tarazi FI, Baldessarini RJ. 2001. Role of dopamine D(4) receptors in motor hyperactivity induced by neonatal 6-hydroxydopamine lesions in rats. Neuropsychopharmacology 25(5):624-632.

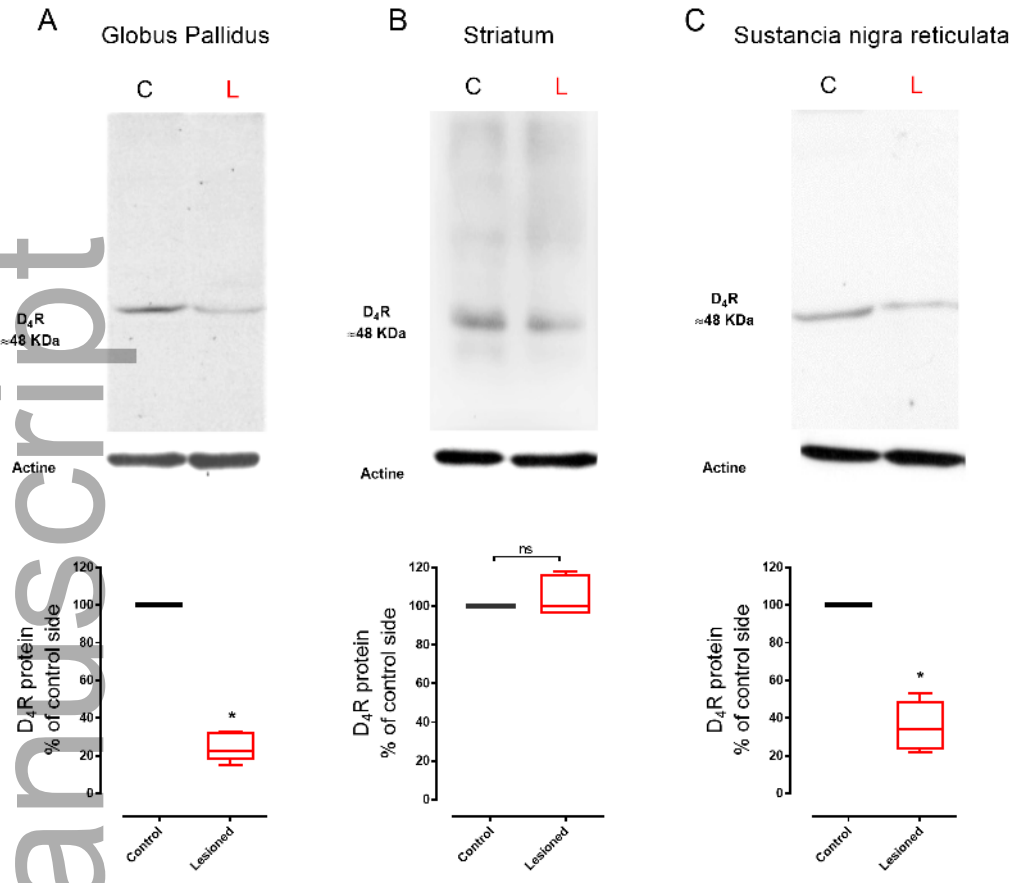

ejn_15020_f1.tif

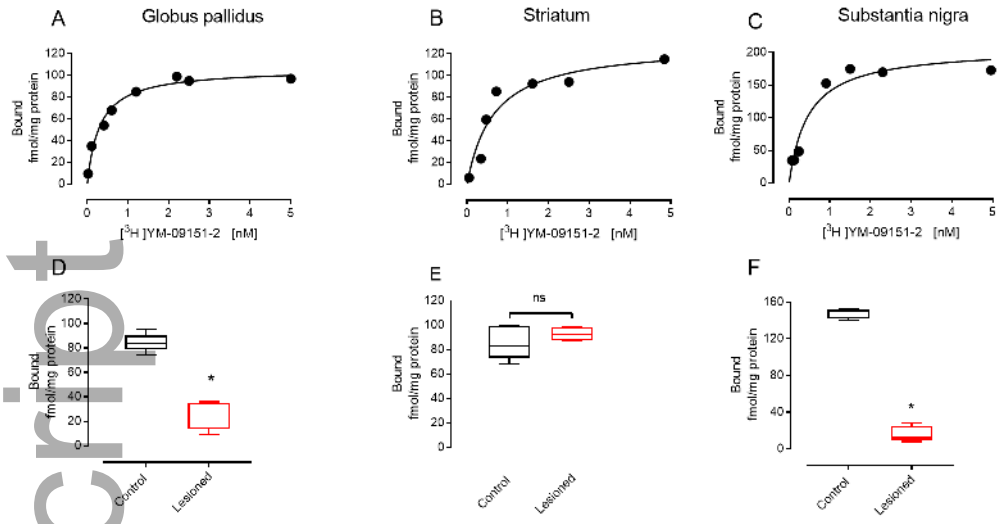

ejn_15020_f2.tif

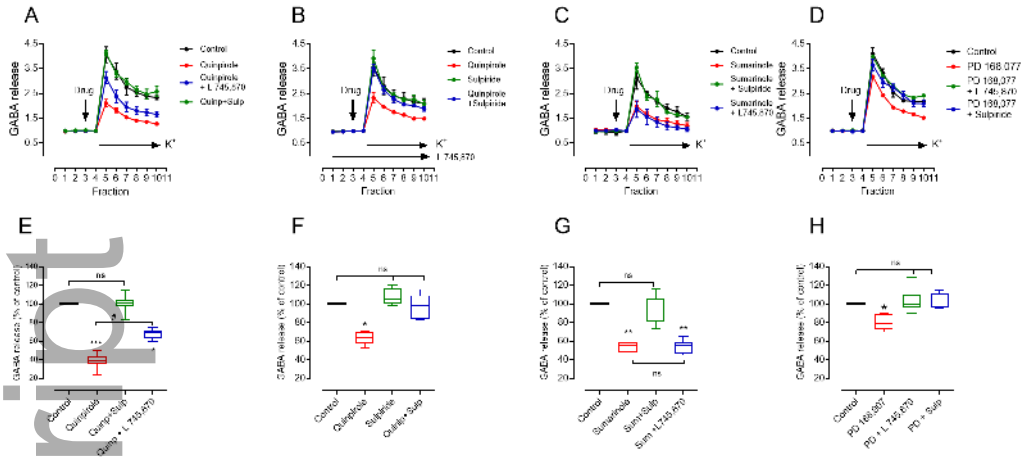

ejn_15020_f3.tif

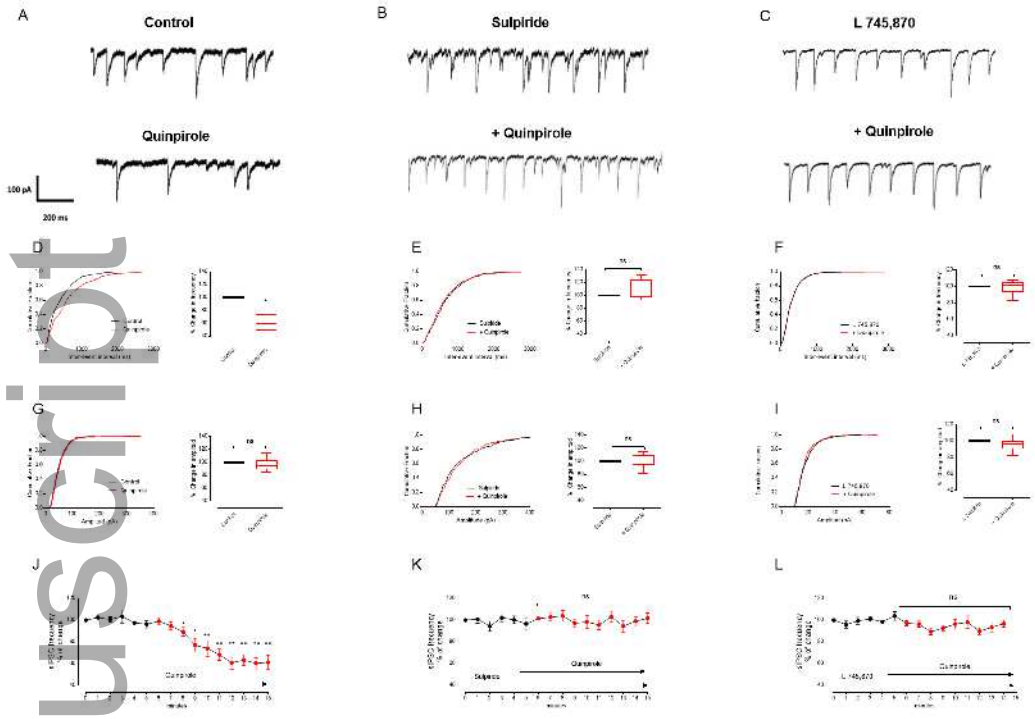

ejn_15020_f4.tif

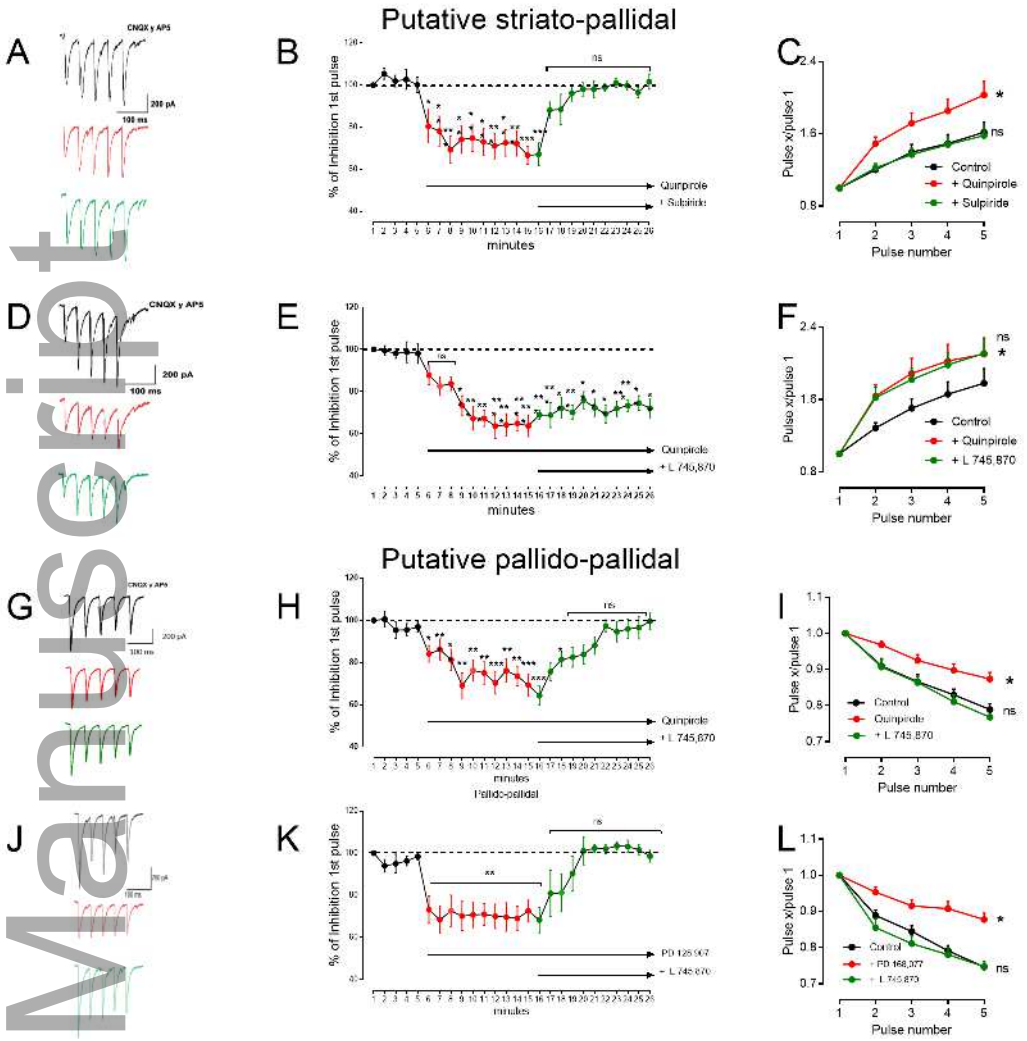

ejn_15020_f5.tif

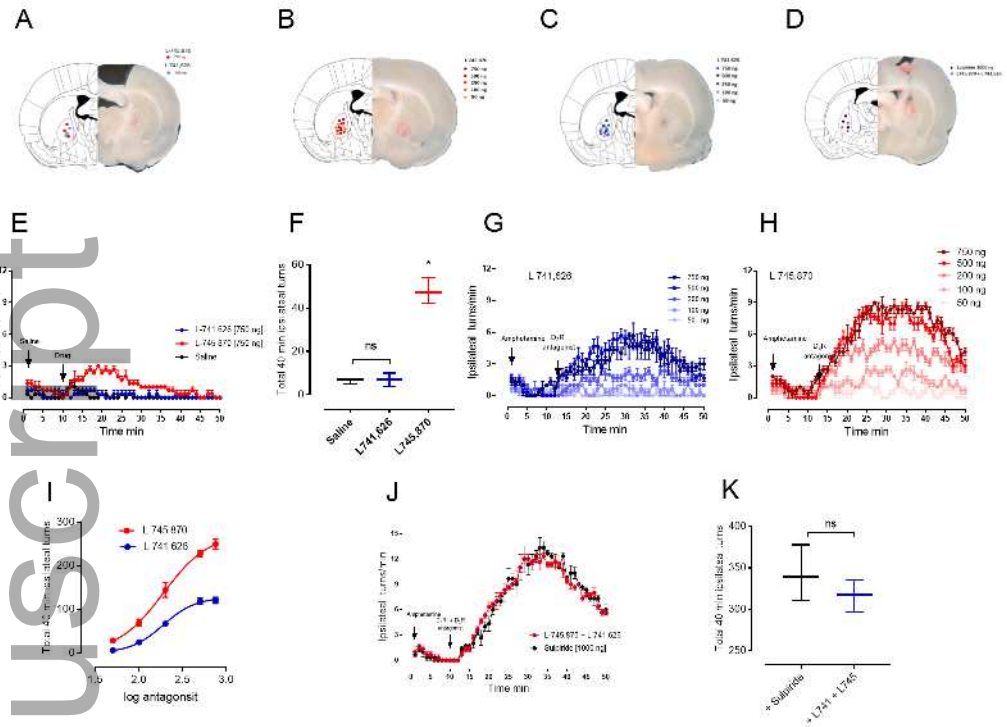

ejn_15020_f6.tif